Politecnico di Milano

School of Civil, Environmental and Land Management Engineering

Master of Science in Civil Engineering-New Structures

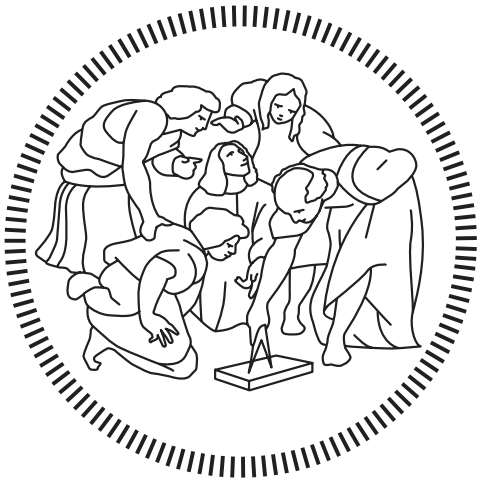

Structural Optimization of Planar and Curved Reciprocal Frames

Supervisor

Prof. Antonio CAPSONI

Candidate

Alessandro BONVINI

Academic Year 2019 – 2020

Abstract

Starting from the aim to reduce the polluting emmisions deriving from the construction processes, in addition to the research on new materials and the improvement of the existing ones, the structural optimization is becoming more significant and used. In this compound the usage of "Reciprocal Frame" was analyzed, for this type of structure it is fundamental the way in which the elements are arranged in order to provide the equilibrium at the frame. The thesis has the aims to understand the structural behaviour of this type of structure and to find the best configuration that is able to reduce the amount of material. The structural behaviour of nexorades was studied for both planar and curved elements in order to understand how these structures behave in their plane and out of it. On the contrary, the optimization was done varying two parameters that are always recalled along the thesis: the engagement length and the macrocell size. In the case of planar reciprocal frame it was used for the optimization a *MatLab* script, which is able to find the best configuration varying the above variables. While for spatial nexorades it has been studied also the variation of the cross-section along the elements with a parametric software called *Grasshopper* and its plug-in *Karamba*. At the end it has been demonstrated that the optimal configuration recall the regular grid which have complete different proprieties and strengths with respect to the already used structural techniques.

Sommario

Partendo dallo scopo di ridurre le emissioni inquinanti dovute al mondo delle costruzioni, oltre alla ricerca di nuovi materiali e al miglioramento di quelli esistenti, l'ottimizzazione strutturale sta prendendo sempre più spazio e visibilità. In questo ambito si è voluto analizzare l'utilizzo dei "Reciprocal Frame", la peculiarità di queste strutture sta nella configurazione con la quale sono realizzate, dalla quale dipende il loro stato di equilibrio. La tesi ha lo scopo di approfondire e studiare il comportamento strutturale di questo tipo di strutture e di ottimizzarne la configurazione in modo da ridurre il quantitativo di materiale utilizzato. Il comportamento da un punto di vista strutturale è stato studiato sia per elementi piani, sia per elementi curvi, analizzando le azioni derivanti dalla componente assiale e da quella flessionale. Mentre l'ottimizzazione è stata effettuata variando i due parametri principali richiamati spesso lungo lo studio: la grandezza delle macrocelle e il rapporto di sovrapposizione. Per i "Reciprocal Frame" piani l'ottimizzazione è stata eseguita con un codice *MatLab* il quale è in grado di trovare la soluzione migliore facendo variare le due variabili sopra citate. Invece gli elementi curvi sono stati ottimizzati anche considerando la variazione della sezione lungo gli elementi grazie ad un software parametrico chiamato *Grasshopper* e il suo derivato *Karamba*. Infine è stato possibile dimostrare, eccezion fatta per qualche caso particolare, che la soluzione ottimale riporta sempre al caso di griglia, la quale però ha caratteristiche e potenzialità diverse da quelle delle classiche maglie usate fino ad oggi.

Contents

List of Figures

Chapter 1

Introduction

In this first chapter it has been described the main characteristics on which the thesis will be developed adding a quick overview on the existing and ancient reciprocal frames. The aims of the study are the analysis of the structural behaviour and the optimization of the planar and curved reciprocal frames. More in detail it has been tried to cover all the possible aspects and difficulties in the design of these type of structures. The first step was the analysis of planar elements with an approach that was as theoretical as possible in order to understand deeply the critical points and the benefits related to nexorades. The further developments on curved elements are made with a parametric structural software which helps in the calculations, but thanks to the easy variability of the parameters involved allows a complete overview on the problem. In all these steps it has been tried to arrive to an optimal solution which minimize the final cost of the construction, and at the end it has been stated that the optimal configuration has always the same characteristics.

1.1 Concept of Reciprocal Frame

The adjective "reciprocal" means literally "an action involving two people or groups of people who behave in the same way or agree to help each other and give each other advantages". But what does "reciprocal" signify from a structural point of view and what kind of quality does it add to frame structures? As a definition of Reciprocal Frame (or nexorade [2]) it can be used the one given by Popovic Larsen [13]: "structures consisting of linear, curved, flat or inclined elements which support each other and are arranged in a way to form a closed circuit or unit". The main aspect from a structural point of view is that the configuration in the space and the assemble of these

Figure 1.1: Simple example of reciprocal frame

structures is crucial for their equilibrium. Every single element composing the structure is supported by its adjacent element that always acts as support (Figure 1.1).
The biggest advantage of reciprocal structures is that the elements are quite short with respect to the overall span of the structure, this aspect can be very helpful in the construction phase in which the workers can deal with lighter elements that should be hold on manually. Moreover, using a specific configuration of straight elements it is possible to match any possible surface introducing a certain eccentricity between elements; the more the elements composing the structure are short and thin, the more the reciprocal frame is able to fit the base surface. Alternatively, if eccentricities are to be avoided, it is always possible to use curved elements as it is done in the Chapter 4. In that case the elements are all coplanar where the plane is the fitted surface. Concerning the planar reciprocal frames, the geometry is easier with respect to the space structure; it is in fact strictly necessary to define the geometry of one singular macrocell and reproduce it until all the given area is covered. Furthermore reciprocal frames are commonly made by wood, which in light of the environmental challenges currently faced also by the construction industry, and its enhanced production and structural performances (eg. Glulam), it is no longer considered as a poor and ancient material, but it is increasingly recognized as one of the most promising building material for the future. One example of timber structure used also as inspiration in the following discussion is the France Pavilion of Expo 2015 (Figure 1.2), which reflects and also predict the final conclusion on the harmony and functionality of the regular grid; in the project they were used also the same type of concealed connectors described in the subsection 2.3.3.

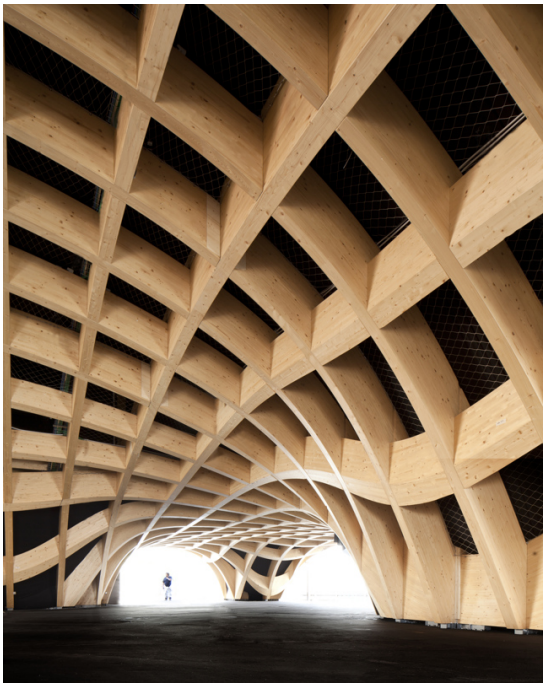

Figure 1.2: France Pavilion Expo Milano 2015

There are two main aspects that must be studied and understood to develop a reciprocal frame design:

- The form finding
- The structural behaviour

1.1.1 Form Finding

While for planar reciprocal frames there are not big problems in the definition of the geometry thanks to the modular definition of the problem, the same cannot be said for spatial reciprocal frame. Indeed, for planar nexorade it is feasible to start from a regular polygon and reproduce it creating a basic grid which will be the starting point of the nexorade.
Once the starting grid is known it is possible to construct inside it the form of reciprocal frame, this process is briefly reported in the Figure 1.3. This procedure creates a continuous structure without discontinuity in the inclination of the elements if the grid is regular, otherwise bent elements will be obtained (Figure 1.3(c)).

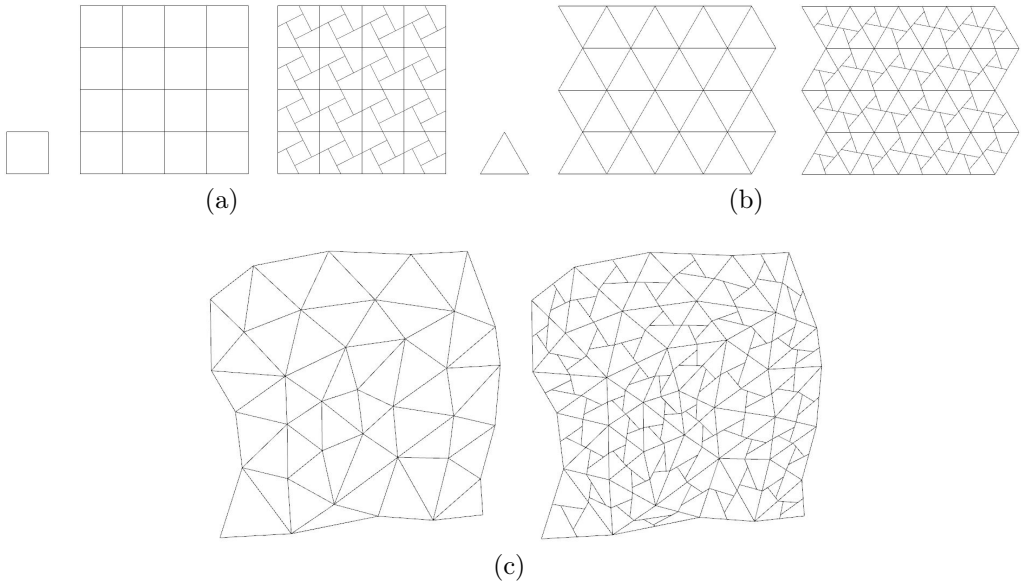

Figure 1.3: form finding procedure of planar RF

The solution with bent element can be rearranged changing the method on which is based on the construction of the RF in order to obtain straight element as in the case of regular grid. However even if from a theoretical point of view it could be a viable path, from an engineering point of view a modular solution whose purpose is to simplify and speed up the erection process, it cannot be done with elements with different length and a chaotic configuration.
For what concerns the 3D reciprocal frame, the problem becomes more complex due to the fact that it is impossible to create a regular grid on a given random surface, and in the case in which a quasi-regular mesh is created, the structure works only if eccentricities between elements are introduced. The eccentricities are needed due to the fact that the cells of the grid are no longer coplanar, so the nexor are now not only bent in the plane of the grid as in the Figure 1.3(c) but also in the space. As it is possible to see in the Chapter 4, one solution can be the use of curved nexor in order to create a smooth surface for the roof. However the problem of elements with different lengths remains.
Just to understand the complexity of the geometry of nexorades, here below is reported an example of the Leonardo's Bridge concept. Even though the structure is not totally three-dimensional, it can be studied considering only the vertical plane; the problem shows the main critical points of the form finding. Indeed it is possible to observe the non-linearity between the ge-

ometry, governed by the thickness of the elements which in turn is strictly related to the structural behaviour.

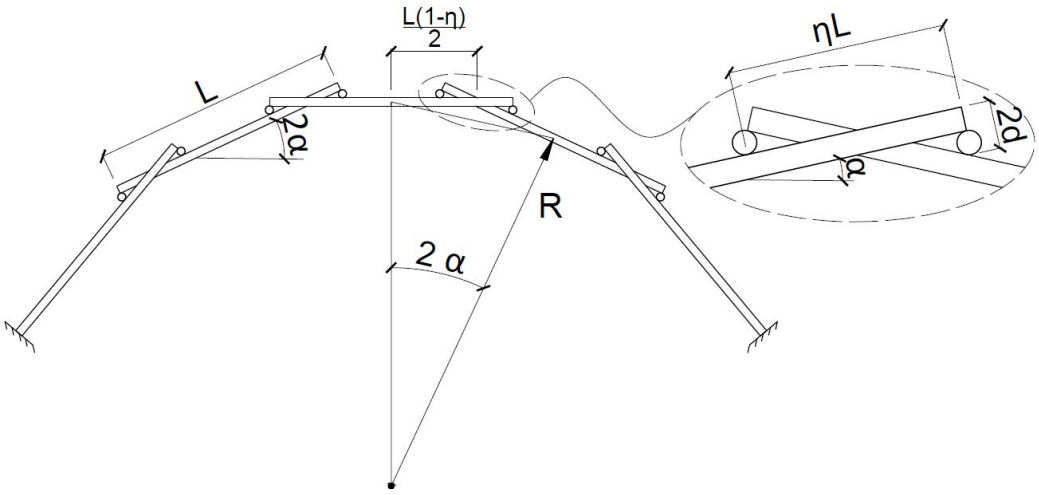

Figure 1.4: Leonardo's bridge geometry

Looking at the Figure1.4, providing as data the length of the elements and the engagement ratio η, and assuming that the shape of the cross-section is circular with a diameter d, it is possible to write the angle α from which the slopes of the elements are obtained.

$$tan\,\alpha = \frac{2\,d}{\eta L} \tag{1.1}$$

$$tan\,\alpha = \frac{L\,(1-\eta)}{2\,R} \tag{1.2}$$

Writing in two different ways the angle and equating the two expressions it has been found the radius R of the circle inscribed into the nexorade.

$$\frac{2\,d}{\eta L} = \frac{L\,(1-\eta)}{2\,R} \tag{1.3}$$

$$R = \frac{\eta\,L^2\,(1-\eta)}{4\,d} \tag{1.4}$$

Figure 1.4 reports the geometry of 2D reciprocal frame also called Leonardo's Bridge, but this planar configuration can be projected out of the plane creating a Barrel Vault Nexorade.
Another interesting example of form finding that can be found in the literature, more specifically on the website *www.albertopugnale.com*[15], is a simple

benchmark on a reciprocal frame configuration made with three elongated elements. He used an optimization algorithm for the form finding of this simple configuration reported in the Figure 1.5 taken from the cited website.

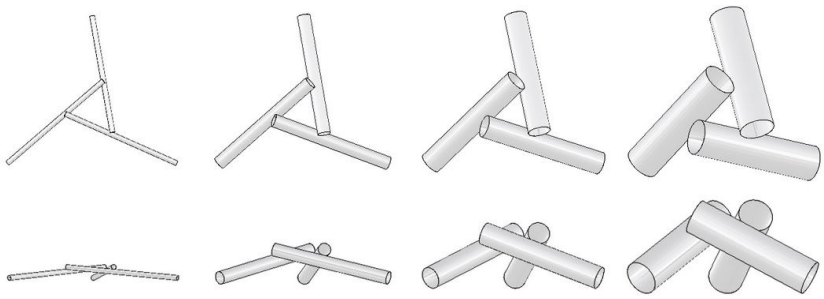

Figure 1.5: Plan and elevation view of reciprocal system with eccentricity

The boundary conditions of the problem are the three support points, the values of the engagement length and the eccentricity which is equal for the three bars. While the design variables are the X,Y and Z coordinates of the three bar ends. The fitness function is defined as a distance between elements, when such a distance becomes zero, the bars will reciprocally lie on one another. The technique used is based on the work done by Bavarel [2] in his doctoral thesis, but the big advantage is that in this case Pugnale has used the package software of *McNeel* which is better described and used in the Chapter 4. In these software are implemented the "Genetic Algorithms" used in this case to minimize the fitness function. More specifically it has been used the "Galapagos" algorithm which does not seem to work optimally even if the problem is quite simple. Anyway it can be noticed how the thickness (or eccentricity) and the engagement ratio of the elements change the configuration increasing the distance from the floor, highlighting the non-linearity in the design process.

1.1.2 Structural Behaviour

The first aspect that stands out is that despite the complex geometry of the reciprocal frames, if the elements belonging to the edges of the surface are simply supported and the connections between elements are designed as hinges, the structure is statically determined. Otherwise, if internal columns or clamped restrains on the edges are introduced the structure becomes statically redundant. However, as it is possible to see in the following chapters, the implementation of an algorithm only based on the equilibrium equations becomes quite complex due to the number of unknowns in the problem also for planar nexorades. Indeed, the theoretical procedure in the world of

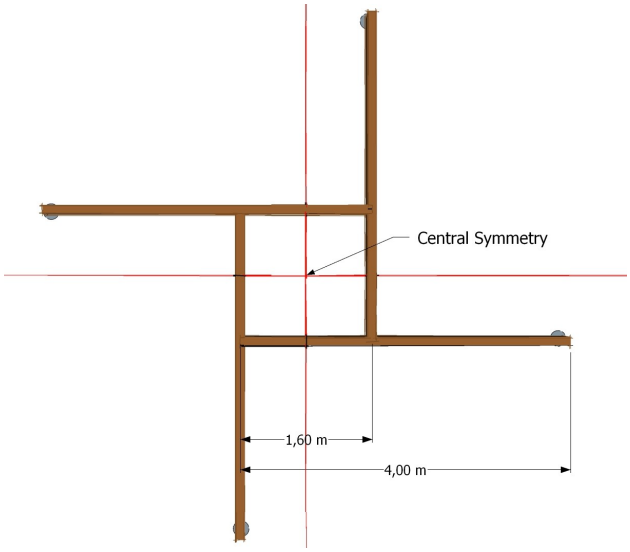

Figure 1.6: Planar geometry of the problem

reciprocal frame is usually avoided, probably because of the complexity of geometrical models and due to the performance and simplicity of modern parametric tools for modelling and analysis.
In order to understand the structural behaviuor of a more complex arrangement of reciprocal frame, here under it is showed a very simple example of only one squared macrocell, with a length element of 4 m, an engagement ratio η of 0.4 (see Section 2.1) and an applied distributed load on each element of 2 kN/m.

$$\eta = \frac{L_{en}}{L} = \frac{1.6\,m}{4\,m} = 0.4 \tag{1.5}$$

To simplify the physics it can be noticed that the geometry and loads have a central symmetry (Figure1.6) such that all the elements have equal generalized actions. In other terms, the vertical force transmitted by one element to its adjacent is equal to the received concentrated load. Writing the equilibrium equation of one element (that can be seen in the Figure 1.7) it is possible to compute the reaction R at the support and the force X that each element passes to its adjacent.

$$R - qL + X - X = 0 \tag{1.6}$$

$$RL - X\eta L - \frac{1}{2}qL^2 = 0 \tag{1.7}$$

$$R = qL = 8\ kN \tag{1.8}$$

$$X = \frac{qL}{2\eta} = 10\ kN \tag{1.9}$$

Since all the applied forces on the beam are known, the shear force and bending moment diagrams can be drawn. The maximum bending moment value can be computed as:

$$M_{max} = X\eta L - \frac{q\,(\eta L)^2}{2} = 13.44\ kNm \tag{1.10}$$

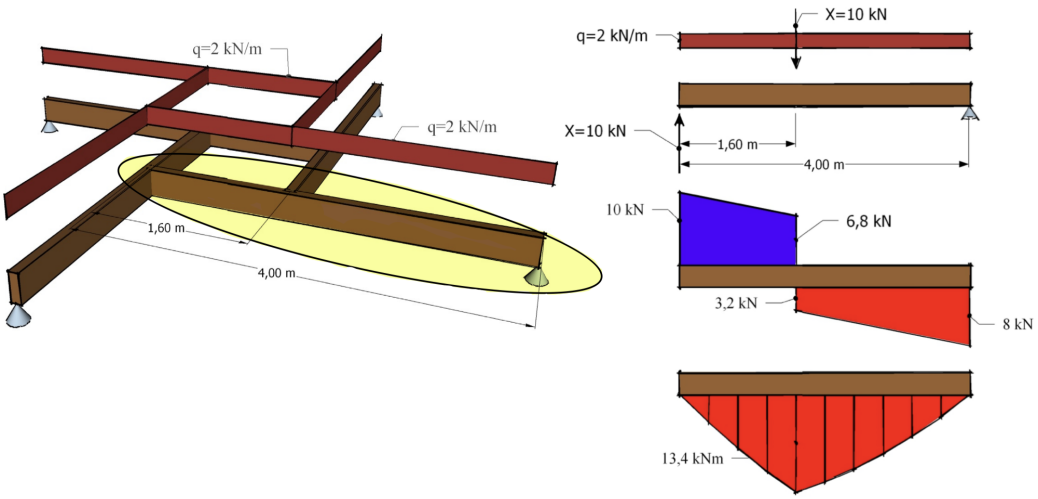

Figure 1.7: Visualization and diagrams of the studied structure

From this simple example it is possible to understand some basics on the structural behaviour of reciprocal frames. The most important is that looking at the Equation 1.9 is possible to derive that the only case in which the structure results statically undetermined is the one in which the engagement ratio is equal to zero, in fact in this case the transmitted force between elements X will increase until infinite. Moreover, looking at the diagrams, it can be noticed that the maximum shear force is in correspondence of the end of the element, while the maximum bending moment is in correspondence of the adjacent element if the applied load is sufficiently smaller than the transferred load from the other element. Otherwise the parabolic diagram becomes preponderant and the maximum moment will approach the midspan of the beam.
For what concerns horizontal loads and more widely the structural behaviour of shell-nexorade hybrids, which is not studied in this thesis, it can be interesting to consider the work done by Mesnil in 2018 [11], who compared a pavilion with or without plates used as bracing system. The result of that study shows that the planar plates stiffen significantly the structure against

horizontal actions reducing up to 8 times the bending moment in the connections.
As a final remark on the structural analysis, in this thesis only linear elastic analysis will be performed. However, in literature it is possible to find studies as the one performed by Garavaglia [5]; studying fibre-reinforced-concrete reciprocal frames, performing a non-linear analysis and considering collapse loads and mechanism, the author derived that reciprocal frames match the collapse behaviour of traditional structures.

1.2 History of Reciprocal Frame

For many reasons it is almost impossible to determine which culture was the first inventor of this structural scheme, or in which century these frames were firstly used. The main reason is that these structures were built with timber and in time deteriorated or were lost due to fire. However, there are evidences all over the world (mainly in the middle east) from thousands of years ago that these structures were known and used.
The pit dwelling, whose origin dates back to the Neolithic age, can be considered as the first example of reciprocal frame in history. However, probably the most famous reciprocal frame is the Eskimo tent belonging to Native American civilization, which is reported in the Figure 1.8 from the book of Popovic Larsen 2008 [12]. The Indian tepee was largely used by the Native American, because it perfectly matched their nomadic lifestyle thank to the fact that the tee can be easily and quickly built.

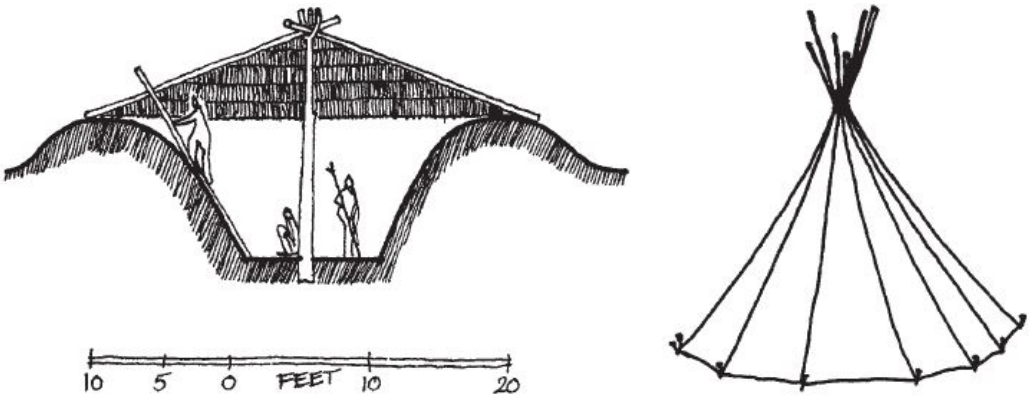

(a) *Neolithic pit dwelling* (b) *Indian tepee*

Figure 1.8: First historical examples of reciprocal frame

Figure 1.9: Rainbow Bridge

Going through the Middle Ages, around the 12^{th} century the Chinese civilization started to use the concept of reciprocal structure for different types of structures, i.e. the bridges. In the Figure 1.9 it is shown a Chinese scroll painting where is represented the "Rainbow Bridge", one of the first reciprocal bridge made of timber.
During the Renaissance Leonardo Da Vinci proposed its own design of a bridge, most probably without influences from the eastern world. The bridge was designed as a temporary structure with a military purpose; its aim was to quickly allow troops to cross rivers. The straight elements are arranged in a way to fit an arch, the shape of the arch depends on the slenderness of every single element and on the engagement ratio. Furthermore Leonardo was the first that developed a planar grillage for floors or roofs. The sketches in the Figure 1.10 are taken from the "Codex Atlanticus".

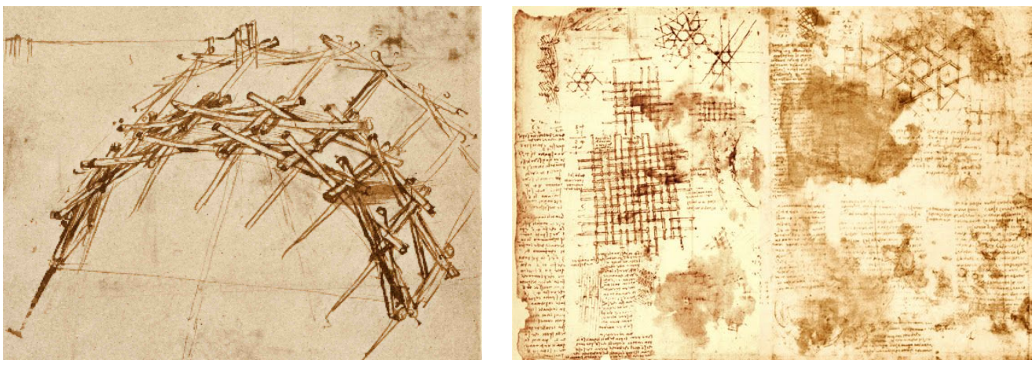

(a) *Leonardo's bridge* (b) *Planar grillage*

Figure 1.10: Codex Atlanticus

Near the sketches, Leonardo briefly introduced the structural behaviour of reciprocal frames. However only in the 17^{th} century, thanks to the mathematician John Wallis, it was described a method based on equilibrium between

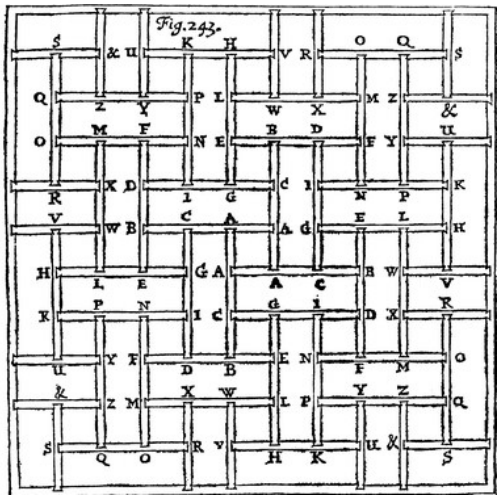

Figure 1.11: The extended structure by John Wallis

elements that computes the forces acting on each element. He presented a clear drawing of the structure in which joints are labelled [10] (Figure 1.11).

In the early 20^{th} century, the German engineer Friedrich Zollinger developed a system of lamella roofing system. This type of structure made with timber was developed and used after the first world war to serve his country in a fast and easy construction for housing.
Until now all the structures showed were composed by timber. This is not surprising. Considering the structural behaviour of reciprocal frame, the elements work in bending and shear and before the advent of steel the wood was the only material possible (even if there were some technique and trials with stones). As it involves the usage of small elements, the reciprocal frame technique was used mainly in the past due to the scarcity of long logs. As time passed the technology has evolved with reinforced concrete and steel to fulfill the aesthetic request. Two main examples are reported in the Figure 1.12, where the Coca-Cola beatbox pavilion in London and the Rokko Mountain Observatory in Kobe, Japan [8] are shown.
The most characteristic example of nexorade is the one used to cover an archaeological site in Burgundy, France, developed by Gelez [6]. The project, being a temporary structure, fulfills the main positives of reciprocal frame, i.e. systematic and simpler erection process, the elements are modular, short and light (they were made by aluminum) and the structure has very low sensibility to settlements. Moreover it can already be seen in this example how the regular grid is a very powerful solution, which simplify a lot also the construction phase.

(a) *Coca-Cola beatbox pavilion*

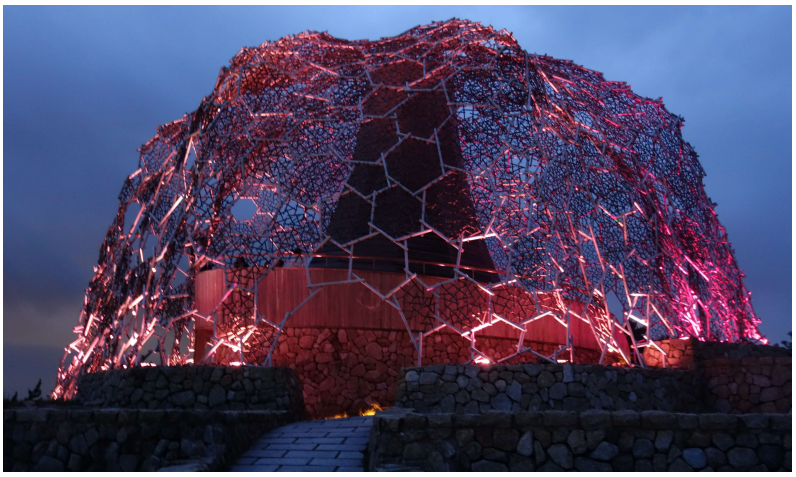

(b) *Rokko observatory*

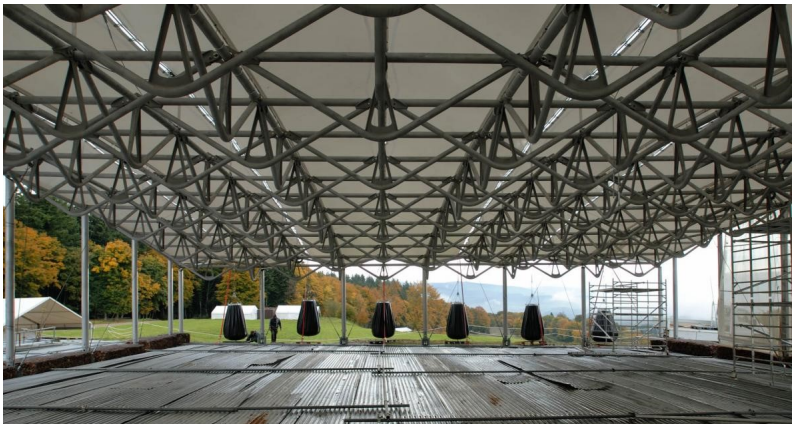

(c) *Burgundy archaeological site*

Figure 1.12: 21^{th} century reciprocal frame

Chapter 2

Quadrilateral Reciprocal Frames

In this chapter a structural analysis model is studied and developed, it is based on the displacement method and it is used for the analysis and the optimization of quadrilateral reciprocal frames in the 2D plane.

2.1 Geometry of Quadrilateral Reciprocal Frames

The geometry of the square quadrilateral reciprocal frame is governed by two main parameters: the width of the square macrocell d, and η that is the ratio between the engagement part of the element and the length of the beam.

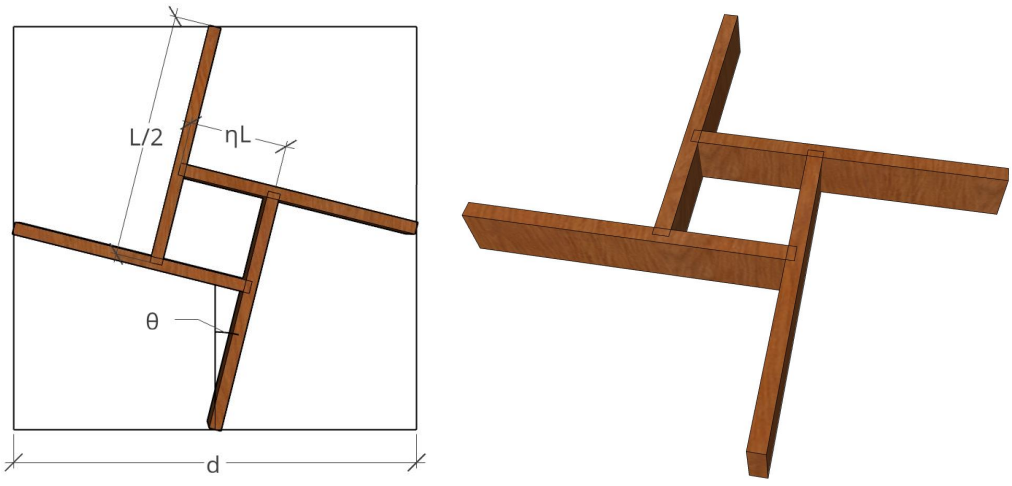

(a) (b)

Figure 2.1: Geometry of quadrilateral macrocell

$$\eta = \frac{L_{en}}{L} \tag{2.1}$$

Knowing these two parameters that should be the data of the problem it can be derived the total length of the beam and the inclination angle with respect to the sides of the covered area. From these information every point in the macrocell can be reconstructed .

$$L = \frac{d}{\sqrt{2\eta^2 - 2\eta + 1}} \tag{2.2}$$

$$\theta = \arctan \frac{\eta}{1 - \eta} \tag{2.3}$$

2.2 Finite Element Method for Quad-RF

In order to solve rapidly the structural analysis of the reciprocal frames varying the η parameter and the number of macrocells for each side, it has been written in *MatLab* a simple script that can compute the maximum generalized actions and displacements, providing as an inputs the Young modulus of the material and the geometrical parameters of the structure and section. The code works only for square macrocells and square covered area, because it assumes the same number of macrocells on each side.
The code is based on the Euler-Bernoulli hypothesis, so it doesn't take into account the shear deformations. Moreover, as it is usually done, also the axial deformation of the elements has been neglected. The finite element is composed by a macrocell; this is different from the usual finite element code, where the finite element is the usual E-B beam. The macrocell, even if it is a planar element in the xy plane, has been idealized for a pratical point of view as a planar element in xz plane, adding 4 fictitious rigid links between the supporting points. The connection between different elements is modelled as a hinge, that can provide also torsional restrain. However the transformation of the planar element in a vertical one, do not consider the torsional degree of freedom of each element, this approximation as it is possible to understand in the followings examples doesn't create big errors in the internal forces for planar reciprocal frames, but it cannot be neglected when spatial structures will be analyzed.
This element has 8 degrees of freedom, but in order to write more easily the stiffness matrix and the nodal force vector using tabulated coefficients, 16 dofs have been used, that later have been cancelled by the static condensation method. The directions of the rotational degrees of freedom are defined in such a way that during the assembling procedure the dofs of two adjacent cells have the same direction. Figure 2.2(a) shows the macrocell element

with its 16 dofs, while in the Figure 2.2(b) only the primary dofs used in the assembling phase are reported.

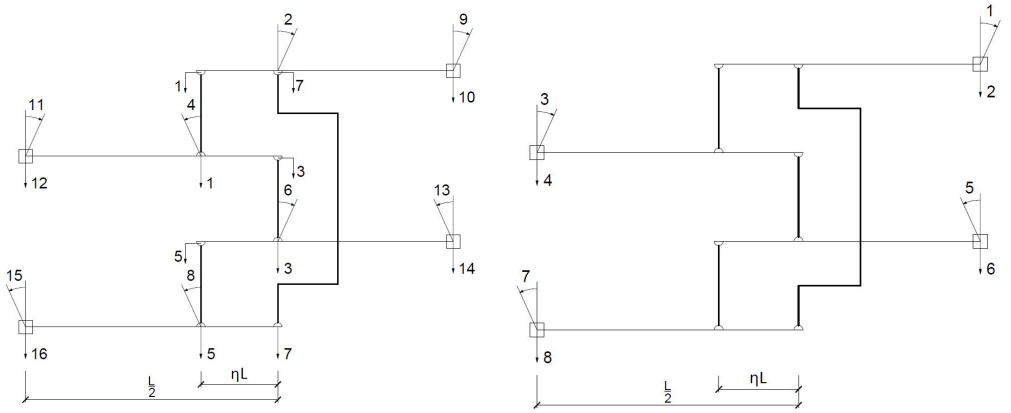

(a) *Primary and Secondary dofs* (b) *Primary dofs*

Figure 2.2: Degrees of Freedom of the Macrocell

Considering these elements loaded by a general uniform distributed load, applying the displacement method the stiffness matrix and the nodal force vector can be derived (Appendix A).

2.2.1 Static Condensation Method

This technique firstly proposed by Guyan (1965) is used for the deletion of unwanted degrees of freedom. It is called static since it doesn't take into account the dynamic effect given by the inertial forces in the equilibrium equations.
Starting from these 16 dofs, the aim is to return to the real degrees of freedom of the cell. This method works if we arrange the degrees of freedom in a proper way. In this case those secondary coordinates are arranged in the first 8 rows, while the remaining 8 primary coordinates are in the last 8 rows. Secondary dofs are those that are intended to be deleted.

$$\begin{Bmatrix} \{F\}_s \\ \{F\}_p \end{Bmatrix} = \begin{bmatrix} [K]_{ss} & [K]_{sp} \\ [K]_{ps} & [K]_{pp} \end{bmatrix} \begin{Bmatrix} \{u\}_s \\ \{u\}_p \end{Bmatrix} \tag{2.4}$$

The vector $\{u\}_s$ lists the displacements corresponding to the secondary degrees of freedom and $\{u\}_p$ is the vector containing the remaining primary degrees of freedom. The system can be solved finding the new stiffness matrix and load vector corresponding to the primary coordinates.

$$[\bar{K}] = [K]_{pp} - [K]_{ps}[K]_{ss}^{-1}[K]_{sp} \tag{2.5}$$

$$\{\bar{F}\} = \{F\}_p - [K]_{ps}[K]_{ss}^{-1}\{F\}_s \tag{2.6}$$

2.2.2 Assembling and Constraints

The assembling procedure is based on the numbering of the nodes that is done for each cell in clockwise direction starting from the top node, while cells are numbered following the traditional convention, going from the left to the right and from the top to the bottom.
For what concerns the constraints, the in-plane displacements are considered fixed. Accordingly, the membrane behaviour of the Reciprocal Frame in this script is not considered. The vertical and rotational displacements can be fixed in any requested node. Assuming supports all along the covered area, the code fixes the vertical displacements on the nodes along the sides of the square.

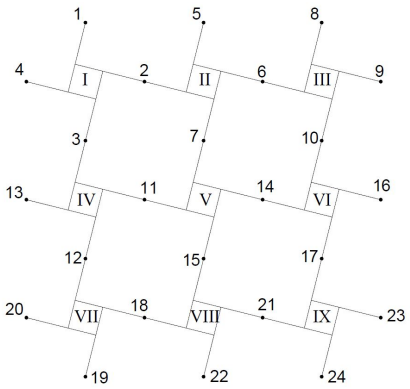

Figure 2.3: Example of numeration of nodes and cells

There are many ways to create constraints in finite element programs. In this case it has been chosen to put zeros all over the columns and rows of the stiffness matrix and in the nodal force vector in correspondence of the constrained degree of freedom except for the jj element of the stiffness matrix. This method works only for fixed restraints. Moreover, the stiffness matrix loses the information to compute the reaction forces. This problem can be overcome assembling in a different way the equations necessary for the calculation of the nodal forces.

2.2.3 Solution of the Linear System and Post-Processing

The solution of the linear system of the equilibrium equations is performed inverting the stiffness matrix by the *MatLab* command backslash which automatically solve the linear system in the most efficient way.
For the calculation of the internal forces it is used a standard post-processing where the stiffness matrix $[\bar{K}]$ and the right hand side vector $\{\bar{F}\}$ of the macrocell only is recalled. The formulation implemented is the following:

$$\{F\}_{el} = [\bar{K}]\{u\}_{el} - \{\bar{F}\} \tag{2.7}$$

Where $\{u\}_{el}$ is the vector listing the nodal displacement of the related macrocell. Starting from the nodal forces of the macrocell, knowing the external force distribution, it is possible to find the maximum values of bending moment and shear force of the macrocell. Since all the maximums of the macrocells are known, it is easy to extract the global maximum that later will be used for designing the reciprocal frame cross-section.

2.3 Design Procedure

The optimal configuration of the reciprocal frame has been carried out considering the following factor:

- The cost of the Timber used for Reciprocal Frame
- The cost associated to the Cross Laminated Timber used to cover the Reciprocal Frame
- The cost of the connections between elements

The material used for the reciprocal frame is the glulam (Glued Laminated Timber), a type of structural engineered wood which consists of several layers of spruce wood glued together in the direction of the grain. More specifically, it is used "glulam GL24h", whose properties are reported in the Table 2.1.

GL24h Parameters	Strength Values [MPa]
Bending strength ($f_{m,g,k}$)	24
Shear strength ($f_{v,g,k}$)	3.5
Modulus of elasticity ($E_{0,g,mean}$)	11000
Shear modulus ($G_{g,mean}$)	4300

Table 2.1: Material parameters

2.3.1 Cross Laminated Timber Design

Cross Laminated Timber (CLT) is a wood panel product made from gluing together layers of solid-sawn lumber. Each layer is placed and bonded crosswise on top of each other. This type of assembling reduces swelling and shrinking to an insignificant minimum level from the point of view of construction technology. Moreover, the finished panel has exceptional thermal insulation propeties and can also dissipate loads in several directions.
The CLT is used to create a plane surface that can be used as floor or roof. The length of the CLT is a function of the parameter η; increasing η the maximum length of the CLT will decrease.

$$L_{CLT} = L\,(1-\eta) \tag{2.8}$$

The design is made considering a unitary width and a minimum height given by the commercial profiles that is 60 mm. The CLT must be designed considering the resistance at ultimate limit state and the deformations in the mid-span. The maximum bending moment and maximum deflection can be computed as follow.

$$M_{max} = \frac{1}{8}\,q_d\,L_{CLT}^2 \tag{2.9}$$

$$f_{max} = \frac{5}{384}\frac{q_d\,L_{CLT}^4}{EI} \tag{2.10}$$

Hence, the height of the CLT is designed as the maximum between the minimum value such that the allowable stress σ_b is not overcome, the minimum value such that the allowable deflection f_{lim} is not reached and the minimum value given by the market.

$$h_{CLT,M} = \sqrt{\frac{6\,M_{max}}{b\,\sigma_b}} \tag{2.11}$$

$$h_{CLT,f} = \sqrt[3]{\frac{5}{384}\frac{q_d\,L_{CLT}^4}{E\,f_{lim}\,b/12}} \tag{2.12}$$

$$h_{CLT} = max\{h_{CLT,M};\, h_{CLT,f};\, 60\,mm\} \tag{2.13}$$

Knowing the geometrical quantities it is possible to compute the total volume used for the CLT and therefore the associated cost.

$$V_{CLT} = A_{tot}\,h_{CLT} \tag{2.14}$$

$$€_{CLT} = V_{CLT}\,€_T \tag{2.15}$$

where the cost of the timber per unit volume $€_T$ is assumed as $1000\,€/m^3$.

2.3.2 Principal Element Design

The first passage to design is the definition of applied loads. In this case it is necessary to pass from the loads per unitary area to loads per unitary length. This passage can be done assuming that the loads are equally distributed on the 4 elements that compose the macrocell as it can be seen in the Figure 2.4. The loads that are taken into account are the self-weight of the CLT and the reciprocal frame structure plus a live load that changes depending on the case studied.

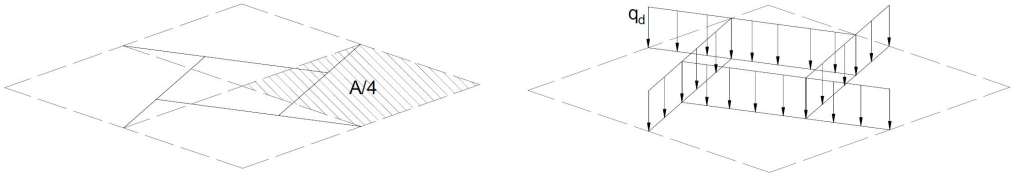

(a) (b)

Figure 2.4: Simplified influence area and distributed load

For what concerns the cross-section of the element it is considered a rectangular shape with a ratio h over b equal to 5. The ratio was chosen because the maximum width for a Glued Laminated Timber is more or less 30 cm and with this ratio it is possible to reach height up to 1.50 m, which can cover quite large spans. Knowing the applied load and the geometry, it is possible to pass at the FEM for quadrilateral reciprocal frame all the parameters that it needs. Once the generalized action M_{max} and T_{max} are known it is possible to compute the minimum height that can resist those actions.

$$h_M = \sqrt[3]{\frac{6\, M_{max}\, h/b}{\sigma_{max}}} \tag{2.16}$$

$$h_T = \sqrt{\frac{3}{2}\frac{h/b\, T_{max}}{\tau_{max}}} \tag{2.17}$$

$$h = max\{h_M;\, h_T\} \tag{2.18}$$

Since all the geometrical data are now known it is possible to calculate the total volume of timber corresponding to the reciprocal frame and the cost of this part of the structure.

$$V_{RF} = L\, b\, h\, n^{\circ}_{el} \tag{2.19}$$

$$€_{RF} = V_{RF}\, €_T \tag{2.20}$$

2.3.3 Connection Design

The connection must respect what it is assumed in the model. In this case with hinged elements, the connection must have an adequate rotational capacity and extremely reduced flexural load-bearing capacity. Moreover, when it is possible, the contact between the elements should be avoided.
In this case in order to certify a certain equivalence between the real cost and the optimization, it is used a type of connection produced by the "KNAPP" company called "Rincon" shown in the Figure 2.6. This type of connector allows for simple and fast joining of the beams, it can be fully concealed and, if needed, a locking clip can be installed to latch the connector.

Figure 2.5: Rincon connectors

To identify the cost varying the load-bearing capacity, the pricelist has been consulted and the prices in the Table 2.2 have been identified.

Article	$F_{2,d}\,[kN]$	€$_{Rincon}$	n° screws	€ for 50 screws	€$_{tot}$
S 140/60	32.26	31.50	7	28	35.42
S 200/60	49.30	33.50	16	28	42.46
S 200/80	68.78	37.80	16	49	53.48
S 290/80	102.78	42.00	25	49	66.50
2x S 200/80	137.57	75.60	32	49	106.96
2x S 290/80	205.57	84.00	50	49	133.00

Table 2.2: Cost of connectors varying the shear capacity

Starting from those values in the Table 2.2 a linear interpolation of the costs can be found. So the linearized formula for the cost is the Equation 2.21, where it is visible a constant part that represents the fixed cost of the connector and a second part of the cost associated to the load bearing capacity.

$$€_{Connectors} = 14\,(1 + \frac{3}{70}\,V[kN]) \tag{2.21}$$

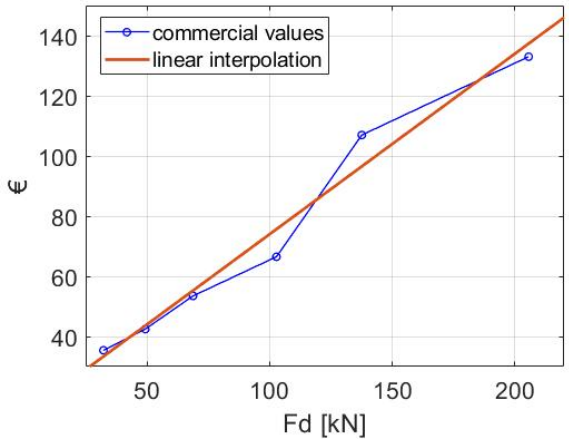

Figure 2.6: Cost of connectors

2.3.4 Design Script

All the previous information are collected in a script that is able to design the sections of CLT and the primary grid computing the total cost of the structure varying the eta parameter and the number of cells at each side of the covered area (n). In the code it is recalled the FEM that is able to calculate the maximum actions on the structure. Moreover the script does not take into account the characteristic values $f_{m,g,k}$ $f_{v,g,k}$ of the bending and shear strength, but the design values $f_{m,g,d}$ $f_{m,g,d}$ computed in accordance with the equation number 4.4.1 of the chapter 4.4 of the italian building code (NTC2018), which is reported here below.

$$X_d = \frac{k_{mod}\, X_k}{\gamma_M} \tag{2.22}$$

Where the coefficient k_{mod} depends on the duration of the load and on the humidity of the structure, while γ_M is the usual material coefficient. A value of $k_{mod} = 0.9$ is used, which considers a small time as a duration of the load, that can be corrected for ultimate limit state, in which it is usually assumed that the structure resists very rarely and shortly to this type of load and an ambient temperature of 20 °C. For γ_M is taken a value of 1.45. With these coefficients it is possible to compute the two design strength:

$$f_{m,g,d} \cong 15MPa \tag{2.23}$$

$$f_{v,g,d} = \frac{k_{mod}\, f_{v,g,k}}{\gamma_M} = \frac{0.9 \cdot 3.5MPa}{1.45} = 2.17MPa \tag{2.24}$$

The symbol approximately equal for the bending strength is used since that value depends also on the height of the beam and it is assumed a sort of average value. Here below are reported two main examples in which the script described is used.

Example 1:

This first example considers a quite small covered area with a side length equal to 8 m. It is taken into account an applied load equal to $5\,[kN/m^2]$ which is totally live load plus the self-weight of the structure where the specific weight of the timber is $4\,[kN/m^3]$. First of all varying the number of macrocells per side, even if the two curves are very attached and for some values of η the cost associated to 3 macrocells is lower than the orange curve, it is possible to see that the cheapest solution is the one related to 2 macrocells for each side.

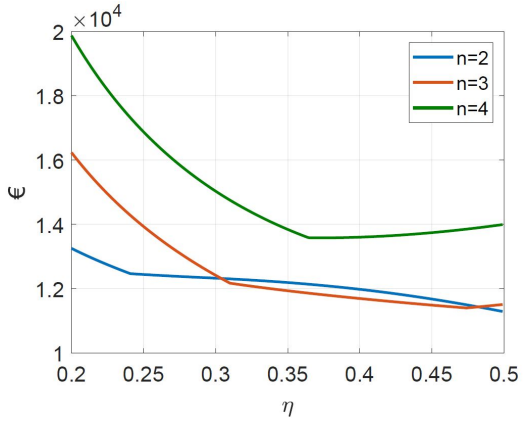

Figure 2.7: Cost of the structure varying n for span length equal to 9 m

Then, analyzing better the case in which n=2, it is possible to understand the optimal η that minimizes the parameter cost. As it is shown in the Figure 2.8(b), even if the curve of the total costs is quite flat starting from η equal to 0.24 until 0.5 (the differences are in the order of 10%) the optimal solution is found for η equal to 0.5.
In the Figure 2.8(b) it can be also appreciated that the cost of the connectors decreases with η. This is due to the fact that the shear force that determines the cost also decreases with η, because with η it is increasing the distance between the support and the applied load of each element and this increases the bending moment, but decreases the shear force. In this case for the optimal η, the reciprocal frame degenerates in a trellis reported in the Figure

2.9. For the optimal solution the principal elements are subjected to a design load $q_d = 11.82\,kN/m$ and the resisting cross-section of the reciprocal frame has a base of 14.5 cm and a height of 72.3 cm, while the height of CLT is 8.6 cm.

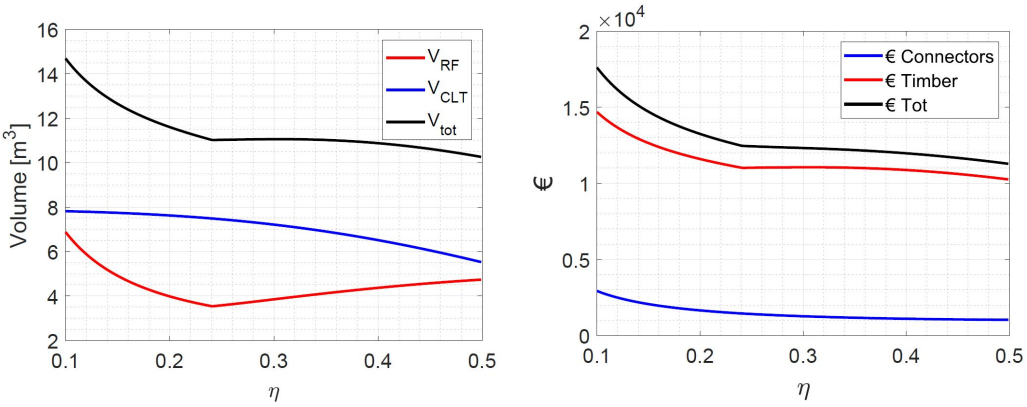

(a) *Timber volume used* (b) *Cost of the structural parts*

Figure 2.8: Volume and Costs curves of the example 1

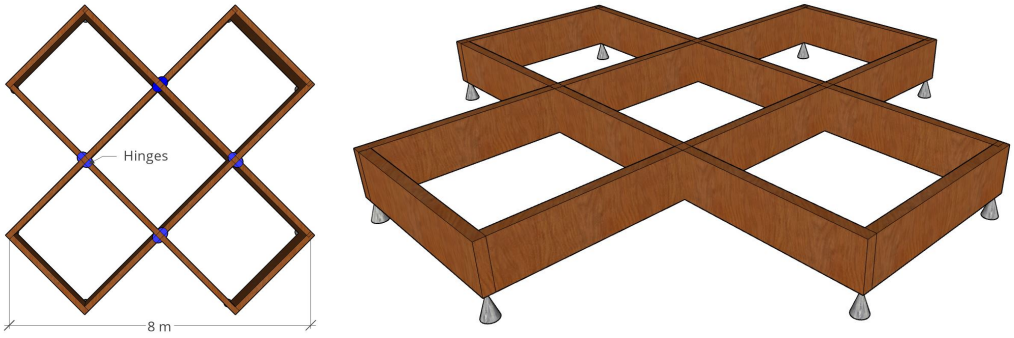

(a) *2D view with hinges* (b) *3D view*

Figure 2.9: Optimal configuration for the example 1

In order to verify the results carried out from the *MatLab* script it is also performed with the same data a finite element analysis with the software *SAP2000*. The main advantage of *SAP2000* is that it automatically constructs the bending moment and shear force diagram which the script does not do, but it finds only the maximum values. In the diagram plotted in Figure 2.10 are reported the bending moment and shear force diagrams, in which blue means positive bending moment and clockwise direction of the

shear force, while in red are plotted negative bending moment and counter-clockwise shear force. The maximum generalized actions of the two methods are written in the Table 2.3, where it can be seen that the differences are very small.

	MatLab [kN]	SAP2000 [kN]
M_{max}	189.10	189.12
T_{max}	83.69	83.58

Table 2.3: Results example 1

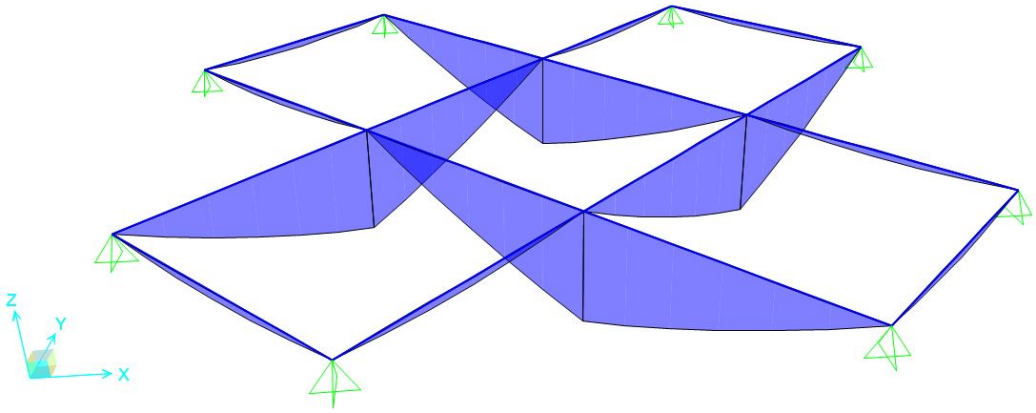

(a) *bending moment diagram*

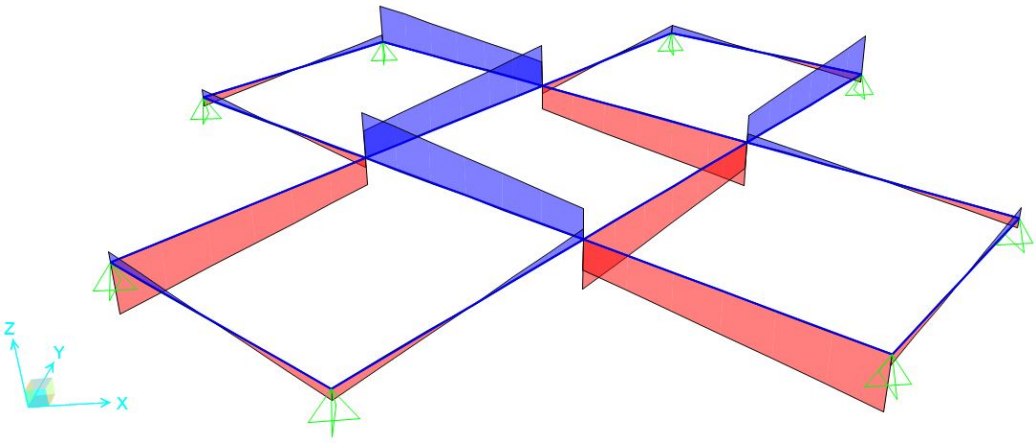

(b) *shear force diagram*

Figure 2.10: Results example 1 by *SAP2000*

Example 2:

In this second example it is considered a roof with a span equal to 16 m; the applied load ($1kN/m^2$) is quite small with respect to the previous case, because as a roof the live loads are usually lower and strictly correlated with the snow loads.
As it is shown in the Figure 2.11 the optimal number of marcrocells for each side is 4, even if as in the previous case two curves are really close.

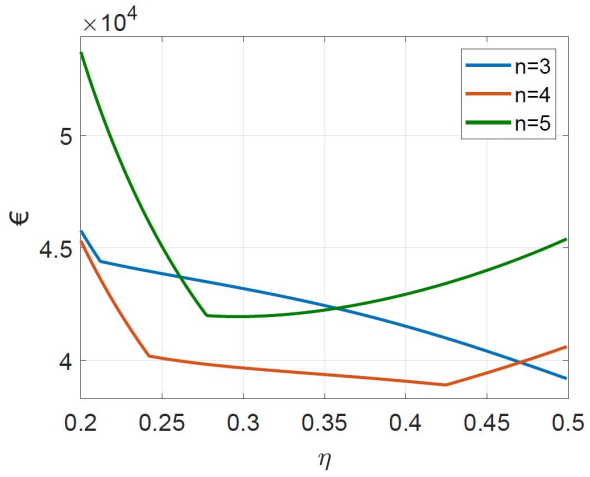

Figure 2.11: Cost of the structure varying n for span length equal to 16 m

Then, analyzing better the case in which n=4, it is possible to understand the optimal η that minimize the parameter cost.

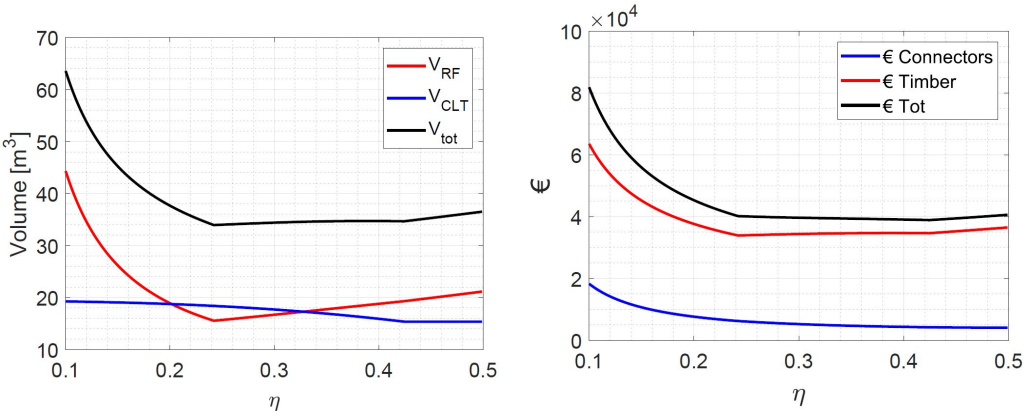

(a) *Timber volume used* (b) *Cost of the structural parts*

Figure 2.12: Volume and Costs curves of the example 2

In the Figure 2.12(a) the curve of the reciprocal frame has two shapes. The first part has an hyperbolic shape and reflects the shear force that in this case governs the design, while in the second part, for larger values of η, the curve becomes a straight line where the problem is governed by the bending moment. For what concerns the CLT, there is a first section until $\eta = 0.424$ where their span can be covered with height larger than the smaller one given by the market, while for the second part the curve becomes flat because the height of the CLT remains constant to $h = 60\,mm$. Looking at the curve of the total costs in the Figure 2.12(b) the optimal solution is reached for $\eta = 0.424$. In the Figure 2.13 it is shown the optimal configuration.
For the optimal solution the principal elements are subjected to a design load $q_d = 3.19\,kN/m$ and the resisting cross-section of the reciprocal frame has a base of 14.7 cm and a height of 73.4 cm, while the height of CLT is 6 cm.

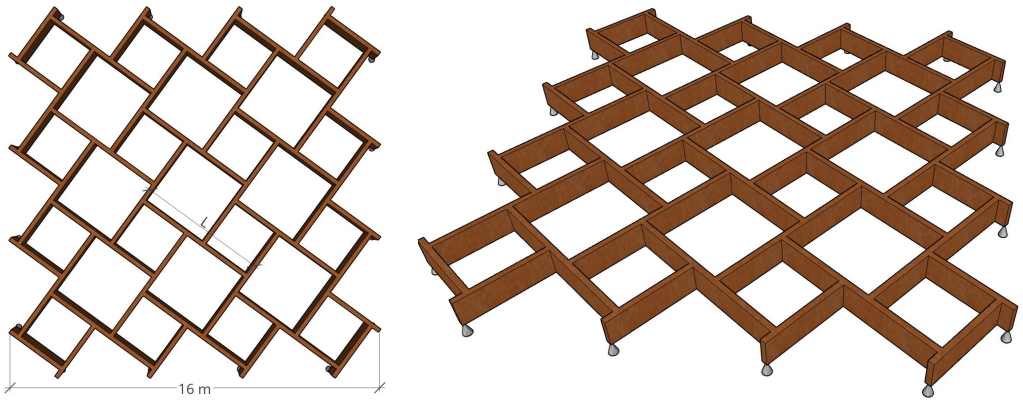

(a) *2D view* (b) *3D view*

Figure 2.13: Optimal configuration for the example 2

Also in this case the results of the optimal solutions are verified with *SAP2000*. The relative diagram that follows the same convention of the example 1 are plotted in the Figure 2.14, while the maximum values are reported in the following table.

	MatLab [kN]	SAP2000 [kN]
M_{max}	197.9	196.68
T_{max}	87.24	86.72

Table 2.4: Results example 2

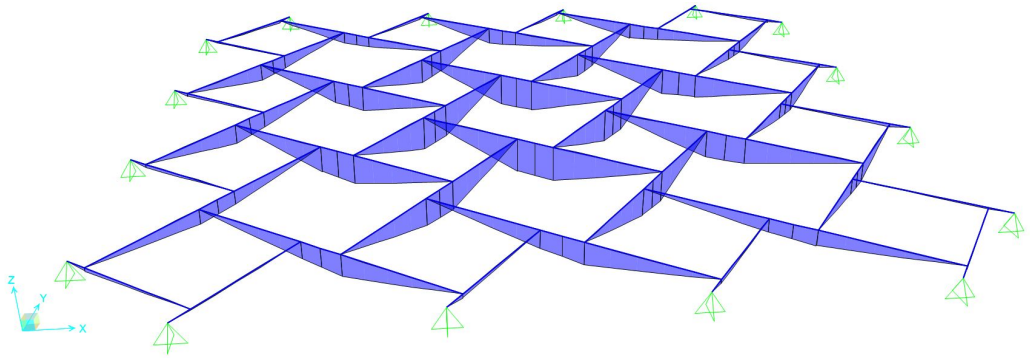

(a) *bending moment diagram*

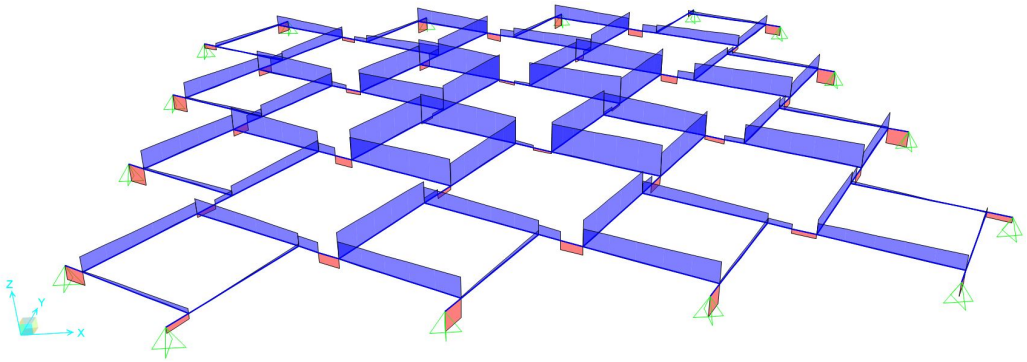

(b) *shear force diagram*

Figure 2.14: Results example 2 by *SAP2000*

In order to have a complete view on the results varying all the parameters involved, in the Appendix B are reported tables in which there are the optimal configurations of the slabs and the main geometrical data of the elements. Moreover it is also reported the total cost of the structural part considering the cost of the timber as $1000€/m^3$ and the cost of the connectors equal to the one computed in the Section 2.3.3.

Chapter 3

Triangular Reciprocal Frames

In this chapter it is analyzed the optimization of triangular reciprocal frames in the 2D plane. The approach used is very similar to the one used for the quadrilateral reciprocal frames.

3.1 Geometry of Triangular Reciprocal Frames

The geometry is no more based on the square's macrocells but on triangular equilateral macrocells composed by three elements with equal length. They can be described starting from two main parameters: the engagement ratio η and the base b of the triangle.

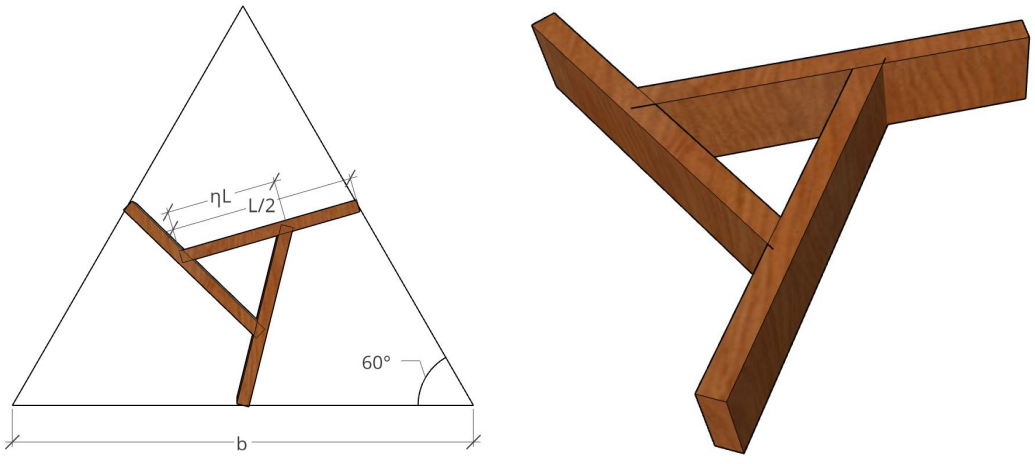

(a) (b)

Figure 3.1: Geometry of triangular macrocell

$$\eta = \frac{L_{en}}{L} \tag{3.1}$$

Knowing these two parameters that can be the data of the problem it can be derived the total length of the beam and the inclination angles α and θ from which it is possible to reconstruct the planar coordinates of any point.

$$L = \frac{b}{2\sqrt{\eta^2 - \frac{3}{2}\eta + \frac{3}{4}}} \tag{3.2}$$

$$\alpha = \arccos\left(\frac{2\eta^2 - \frac{5}{2}\eta + \frac{3}{4}}{(1-2\,\eta)\sqrt{\eta^2 - \frac{3}{2}\eta + \frac{3}{4}}}\right) \tag{3.3}$$

$$\theta = \alpha - 30^\circ \tag{3.4}$$

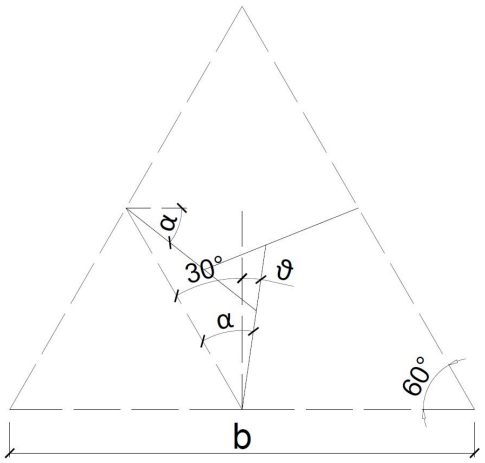

Figure 3.2: Definition of angles

3.2 Finite Element Method for Trian-RF

As in the case of quadrilateral reciprocal frame it is developed a finite element method in order to solve rapidly the structural analysis of the triangular reciprocal frames varying η and the number of macrocells. The code is based on the macrocell showed in the Figure 3.1 so it works only for equilateral triangle. Moreover it is built on the same hypotheses of the Section 2.2, it is able to compute the maximum shear force and bending moment acting on the structure.

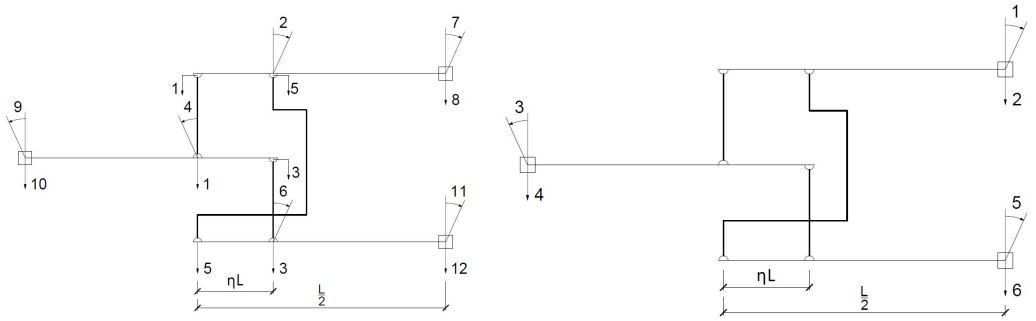

(a) *Primary and Secondary dofs* (b) *Primary dofs*

Figure 3.3: Degrees of Freedom of the Macrocell

The macrocell is idealized as a combination of E-B beams elements connected by 3 fictitious rigid links between supporting points as we can see in the Figure 3.3, the connections between beams are modelled as hinges which can provide also torsional restraint. This macroelement has 6 degrees of freedom but in order to write the stiffness matrix and the nodal force vector easily six additional degrees of freedom have been introduced, which were later deleted with the static condensation method described in the Section 2.2.1. In the Figure 3.3(a) is reported the macrocell with both primary and secondary dofs and in the Figure 3.3(b) are reported only the primary degrees of freedom later used in the assembling procedure. Moreover considering a uniform distributed load applied on all the elements, it is possible to write the stiffness matrix and the nodal force vector (Appendix A).

3.2.1 Assembling and Constraints

The assembling procedure is based on the numbering of the macrocell within the overall slab. In order to simplify the procedure and to create semi-squared elements it has been assembled two macrocell as it is shown in the Figure3.4. Using this element as reference, it is used n to identify the number of cell of this type for each side.
Differently from what it is done for the quadrilateral RF in this case it is not possible to choose a configuration of the rotational degrees of freedom such that they are in the same direction in two adjacent macrocells. So it is take into account during the assembling procedure this fact, changing opportunely in the global stiffness matrix and in the global nodal force vector the signs of those mixed coefficients. The numbering of the macrocell is done using as a reference, the direction in which is oriented the macrocell shown in the Figure

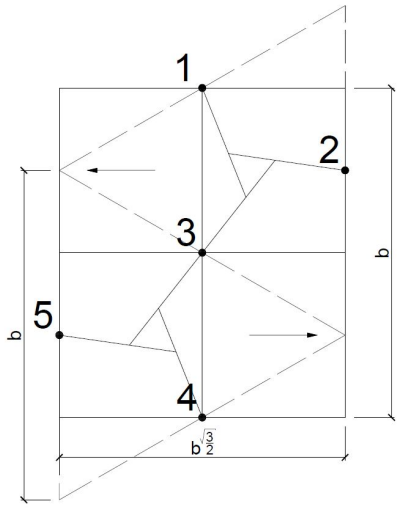

Figure 3.4: Cell type for assembling with numbering of nodes

3.4 with an arrow, from that direction, the numbering is done in clockwise direction.
Taking into account that the in-plane displacements are considered fixed, the others displacements can be fixed wherever is necessary. The code fix the vertical displacement of the nodes on the edges of the slab considering those edges as a simple supports. The procedure that is used in the script for apply those constraints is the same of the one reported in the Section 2.2.2, as well as for the system solution and the post-processing the procedure used in the Section 2.2.3 is reproduced for this case.

3.3 Design Script

The optimal configuration of the slab has been carried out considering the same factors, materials, connections and procedures used in the Section 2.3. One little difference is the length of the cross laminated timber used to create a floor area. In this case the equation is the following:

$$L_{CLT} = \sqrt{3}\, L\, (1 - \eta) \tag{3.5}$$

The second difference is that, due to the configuration of the macrocell from which is build the script, the covered area cannot be squared but rectangular with a ratio between the two edges equal to:

$$\frac{L_2}{L_1} = \frac{\sqrt{3}}{2} \tag{3.6}$$

$$b = \frac{L_1}{n} \tag{3.7}$$

Where the L_1 is the largest length from which is obtained the width "b" of the triangle and n is the number of cells type for each side. In the case in which it is given a square area it is possible to elongate only those elements near the edges in the shortest direction and verify if they can resist at that additional loads that for sure are present due to the larger values of the lengths. Luckly those elements are the ones less loaded (see Figure 3.8).
Here below are reported two main examples: the first one considers a small covered area with maximum span of 8 m but quite high loaded ($5kN/m^2$), while the second example considers an higher covered area with a maximum length of 16 m but less loaded ($1kN/m^2$).

Example 3:

In this example of triangular reciprocal frame it is considered a covered area of 8x6.93 m and an applied live load of $5kN/m^2$, while the self weight of the structure is intrinsically computed by the code.
The first optimization is done varying the number of cell type and the result plotted in the Figure 3.5 shown that the cheapest solution is reached for n=2.

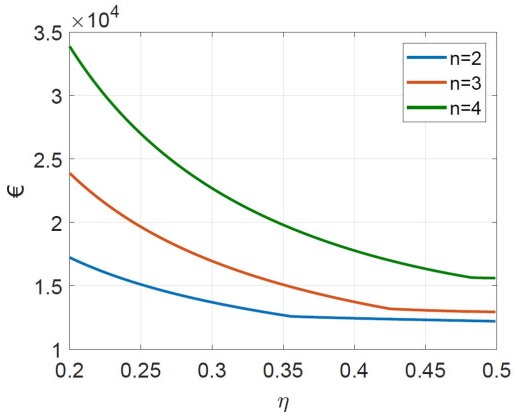

Figure 3.5: Cost of the structure varying n for L_1 equal to 8 m

Then analyzing better the case in which n=2, it is possible to see how the cost of secondary elements i.e. the cross laminated timber is governing the problem while the cost of the connectors is low since the number of macro-cell is really small (only 8). As in the case of quadrilateral reciprocal frames the design of principal elements is governed by the shear force for η small while for η larger than a certain value the shape of the curve change and the

bending moment becomes preponderant. In this specific case the optimal solution is reached for $\eta = 0.5$ where the reciprocal frame degenerates in a trellis reported in the Figure 3.7.
The cross-section of primary elements subjected to a design load $q_d = 9.83\,kN/m$ has a base of 13.6 cm and an height of 68.2 cm while the CLT height is 10.6 cm.

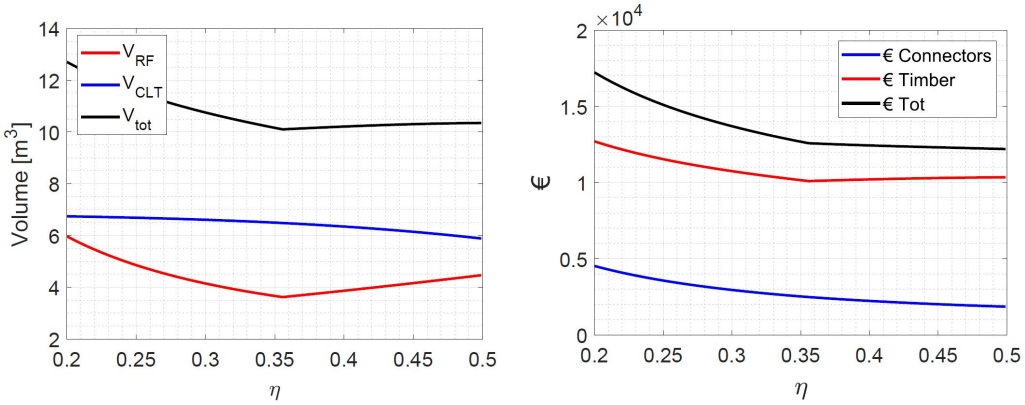

(a) *Timber volume used* (b) *Cost of the structural parts*

Figure 3.6: Volume and Costs curves of the example 3

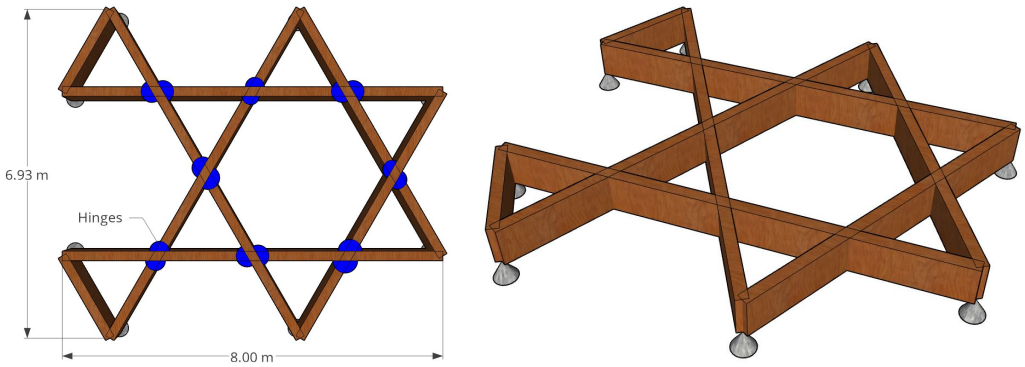

(a) *2D view with hinges* (b) *3D view*

Figure 3.7: Optimal configuration for the example 3

As in the case of quadrilateral reciprocal frame the results for the optimal solution, in which $\eta = 0.5$, have been verified with a finite element program. The diagram and the maximum applied actions are reported respectively in the Figure 3.8 and in the Table 3.1.

	MatLab [kN]	SAP2000 [kN]
M_{max}	158.76	159.15
T_{max}	89.42	89.41

Table 3.1: Results example 3

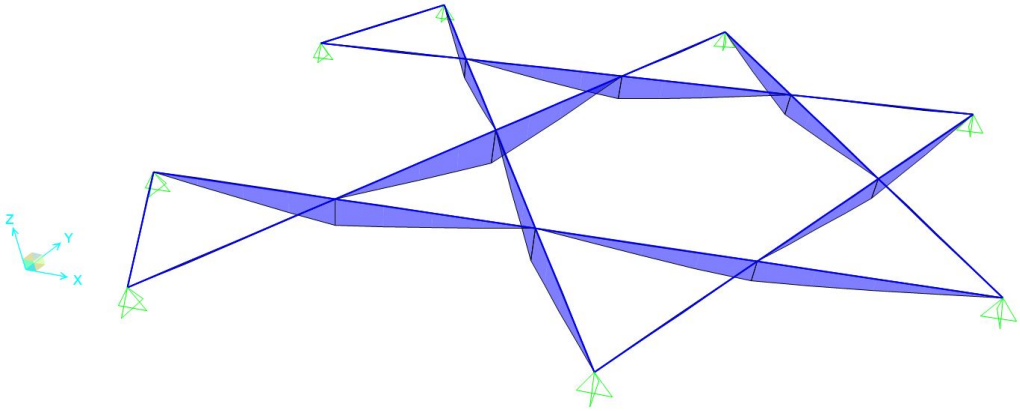

(a) *bending moment diagram*

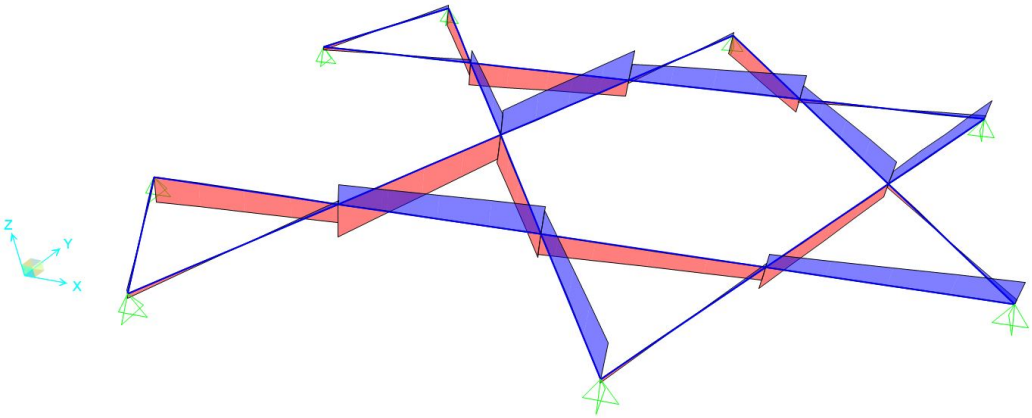

(b) *shear force diagram*

Figure 3.8: Results example 3 by *SAP2000*

Example 4:

This example considers a covered area of 16x13.86 m with an applied live load of $1kN/m^2$. Given this great span and low load, this example can be correlated with a roof of a pavilion. Analyzing the optimal number of cell type it has been found an n_{opt} equal to 4 (see Figure 3.9.

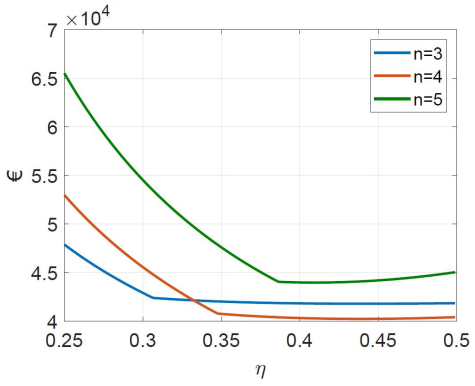

Figure 3.9: Cost of the structure varying n for L_1 equal to 8 m

Focusing on the case n=4 it is possible to find the value of η_{opt} that in this case is 0.418, differently from the previous example here the principal elements are preponderant in the definition of the total volume, in fact it has been obtained a value of η different from 0.5. The cross-section that resists at the maximum bending moment and shear force generated by a design load $q_d = 2.86\,kN/m$ with a ratio height over base equal at 5 has a base of 13.6 cm and an height of 68.1 cm, while the CLT has a thickness of 7 cm.

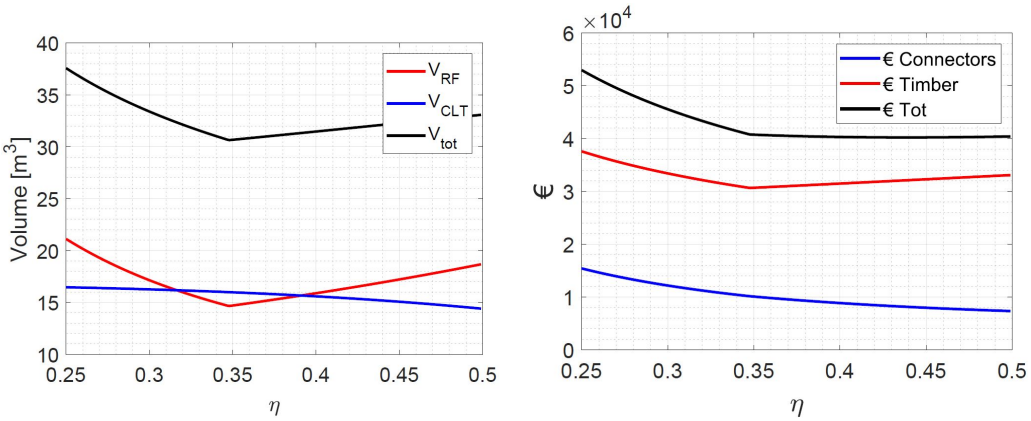

(a) *Timber volume used* (b) *Cost of the structural parts*

Figure 3.10: Volume and Costs curves of the example 4

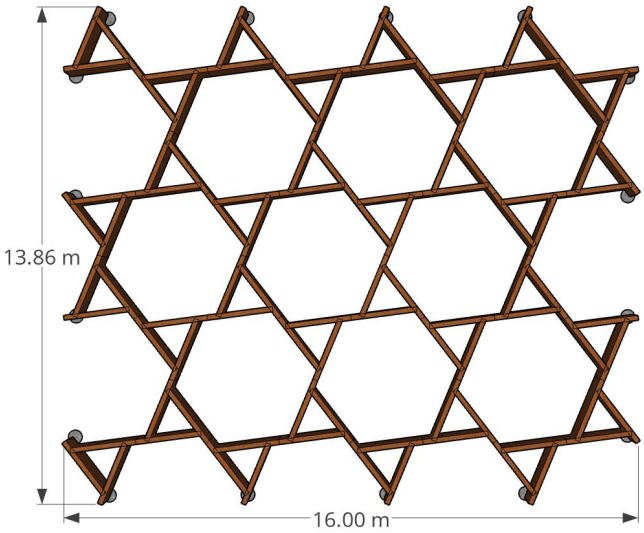

(a) *2D view*

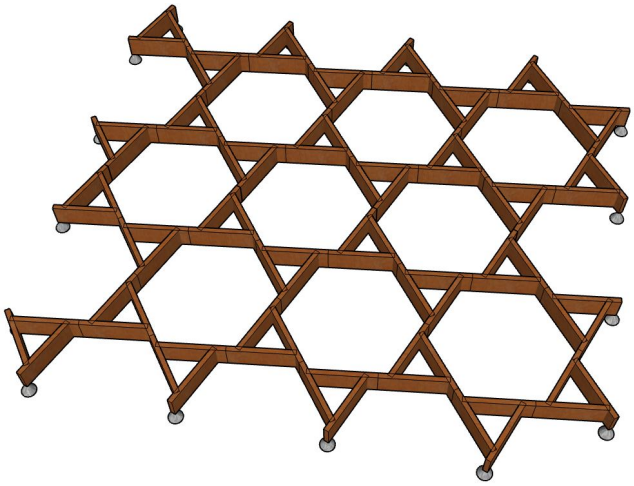

(b) *3D view*

Figure 3.11: Optimal configuration for the example 4

Even for this last example of planar nexorade, they are verified the results carried out from the *MatLab* script. The diagram of the bending moment and the shear force are reported in the Figure 3.12, while in the Table 3.2 it is possible to find the maximum values coming from the two different methods, in this case the differences are always less than 5%, but are larger with respect to the other cases, this fact can be blamed to the hypotheses made in the *MatLab* script, i.e. it was neglected the torsional effect on the slab, that in this case affects in a small amount the results. Moreover it can be noticed that these errors are on the safe side of the problem.

	MatLab [kN]	SAP2000 [kN]
M_{max}	158.25	153.54
T_{max}	105.48	101.89

Table 3.2: Results example 4

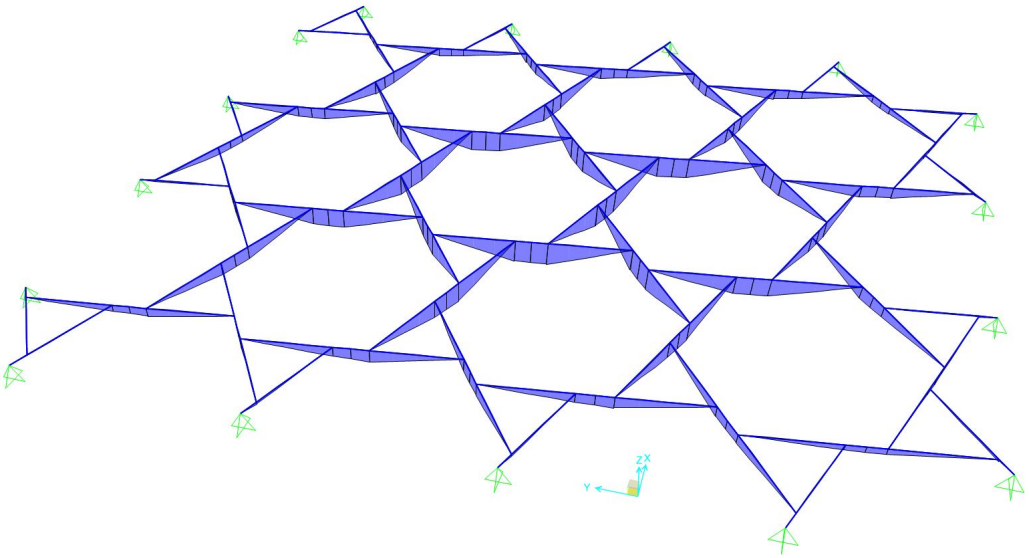

(a) *bending moment diagram*

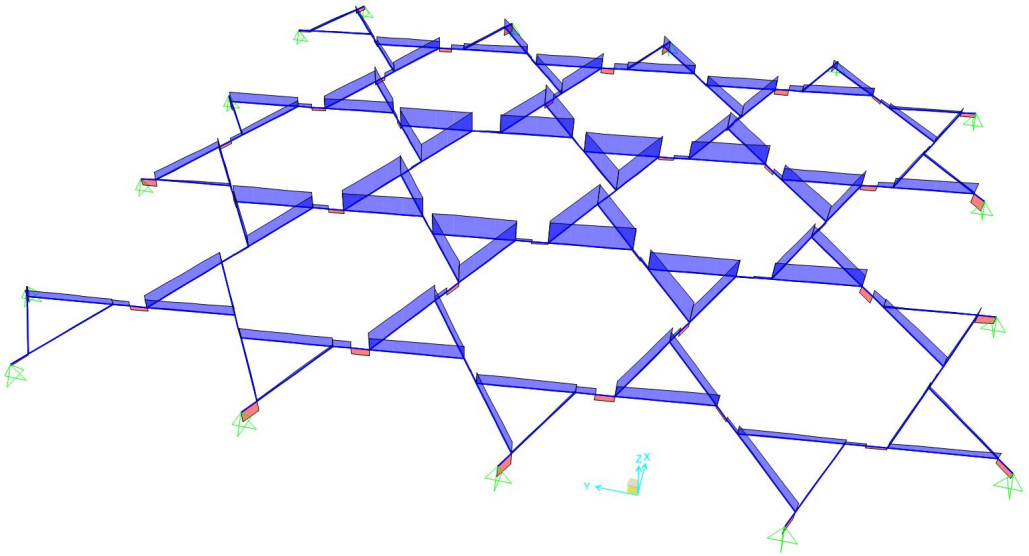

(b) *shear force diagram*

Figure 3.12: Results example 4 by *SAP2000*

As a general remark, on the basis of these examples can be asserted that the costs related to the triangular reciprocal frames are slightly higher with respect to the ones connected to the quadrilateral reciprocal frames even if the covered area of the triangular RF is smaller than the other one. This rule is always satisfied in the results reported in the Appendix B. However with the triangular RF is more frequent the situation in which it is obtained a η_{opt} different from 0.5, which should be more esthetics.

Chapter 4

Spherical Reciprocal Frames

In this chapter three-dimensional reciprocal frames have been studied and optimized, more precisely: semi-spherical domes. Since the complex problem related to the form finding of spatial nexorade, the usage of normal finite element program, or *MatLab*, is not more easy and sensible, so it has been decided to use the *Rhinoceros CAD* environment strictly connected to the plug-in *Grasshopper* in order to control parametrically the design of reciprocal frames in three dimensions. For what concern the structural analysis of nexorades it has been used a parametric structural engineering tool which provides accurate analysis of spatial trusses, frames and shells, that works in the environment of *Grasshopper*, called *Karamba3D* [14].

4.1 Geometry of 3D Reciprocal Frames

As it was said previously in the Section 1.1.1 the definition of three-dimensional reciprocal frames should be quite complex, and it is even more complicated if the geometry is defined parametrically as it is done. In order to simplify a bit the problem, focusing more on the structural part, it is introduced the usage of curved element, this design option it is done mainly to avoid eccentricities between elements, but also to create a smooth surface for ceiling.
The *Grasshopper* environment for structural problems works in a way in which, before it is defined with lines and curves the basic geometry, and then this lines become a beam elements with the tools of *Karamba*. So first of all it was defined a planar reciprocal frame geometry in a slightly different way with respect to what was done in the Chapter 2 and 3, however also in this case the planar geometry has been parameterized varying the size of the macrocell and the engagement ratio eta. Moreover the algorithm constructed in *Grasshopper* (Figure 4.1) for the definition of reciprocal frame can work

with any type of polygon in input.

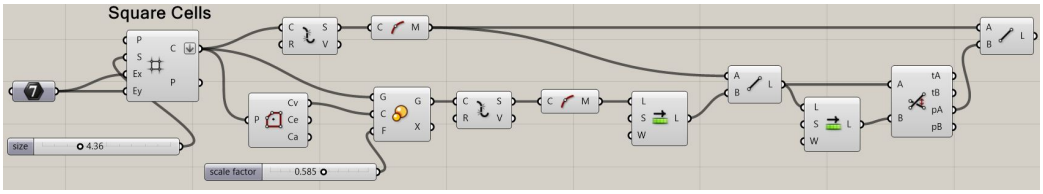

Figure 4.1: *Grasshopper* algorithm for constructing planar reciprocal frame

Then it was defined the surface on which the planar nexorade was projected, in this case as a three-dimensional surface was chosen the lowered dome, also the dome is parameterized varying the radius and the height. The power of *Grasshopper* is that all these variable can be changed easily such that the geometry change automatically without any redrawing or further definitions.

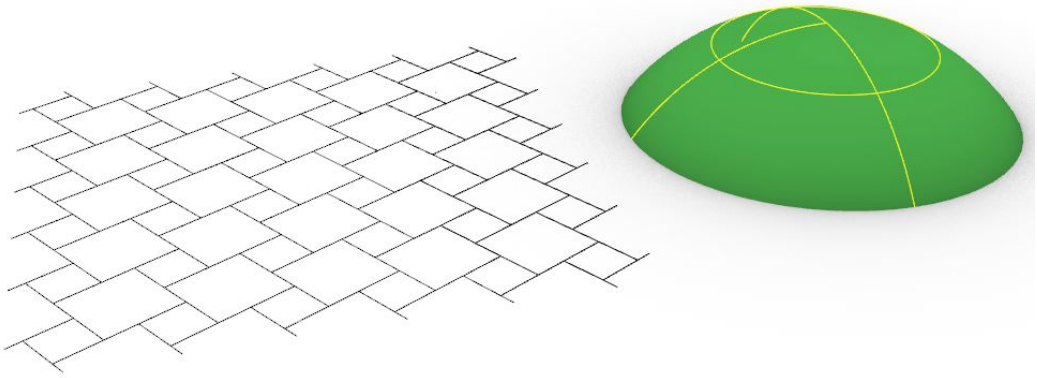

Figure 4.2: Base geometries

When the two base geometries are defined the lines of the reciprocal frame were projected on the lowered dome, the projection rule can be changed in order to minimize the distortions connected to it, in this case a vertical projection was chosen. Before passing the curves to the structural tool *Karamba*, it is necessary to make a comment on it, in fact the analysis component made by *Karamba* works only with straight lines, so the actual curves belonging to the lowered dome have been split at their intersection and then divided in a number of segments such as the differences between the real curve and the piecewise line are negligible. This type of projection used to construct the nexorade on the lowered dome can be done with any type of surface that could be studied, obviously it must be taken into account that with this type of projection more the surface is vertically, more the distortion will increase.

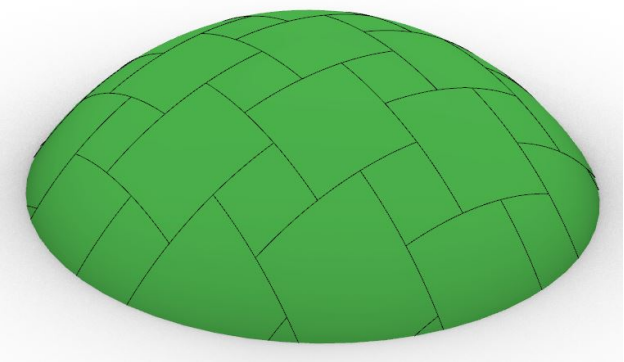

Figure 4.3: Projected reciprocal frame

4.2 Structural Analysis with *Karamba3D*

Once the geometry to analyze is defined, it can be passed to the component "Line To Beam" of *Karamba*, this component finds out how the input (lines) connect between each other and outputs beams as well as a set of unique points which are their end-points.
Since *Grasshopper* works without physical quantities, but thinks in units, it is important to highlight that each unit corresponds in *Karamba* as a meter. Moreover even if it is not crucial in the assembling procedure as in other finite element programs, it is important to mention the orientation and the reference system of the beams, also because it is useful in the post-processing phase. In *Karamba* the default orientation, that can be also changed with specific components, of the local coordinate system of a beam follows these conventions:

- The x-axis starts from the starting-point and finishes to end point following the beam axis
- The y-axis of the beam is at right angle with respect to the x-axis and parallel to the global xy-plane, in the case in which the local x-axis is perpendicular to the xy-plane the y-axis of the beam is chosen parallel to the global y-axis
- The local z-axis is defined starting from the other two axes following the right-handed coordinate system

Before the assembling procedure must be defined supports, joints, materials, cross-sections and loads. For each of these quantities there is a specific component that generates it in *Karamba*. For example the joint component is used to release some degrees of freedom at the connection, because the default

settings impose a rigid connection between two or more intersected elements. The assemble component collects all the necessary information and creates a statical model from the inputs. Once the statical model is defined it can be used the component "Analyze" in which the first order finite element analysis is performed, this component of *Karamba* computes the displacements and the internal forces of the structure neglecting the influence of the axial force in the stiffness of the elements. Alternatively it can be performed, always with a tool of *Karamba*, a second order analysis of the reciprocal frame, the component compute the second order axial force with an iterative procedure with repeated updates of N_x^{II}. In order to make the post-processing and visualize the results there is another component called "Beam View" which allows to visualize in *Rhino* the diagram of internal forces, the deformed shape and the normal stresses of the cross-section.

4.2.1 Structural Behaviour of Spatial Reciprocal Frames

Here below, starting from a general example, it has been wanted to emphatize the main key features of the structural response of spatial reciprocal frame. So it is studied as a general example a quadrilateral base geometry with a size of macrocell equal to 4.5m and an engagement ratio $\eta = 0.375$, projected on a lowered dome with a radius of 10m and an height of 5m. The applied load for unitary area is $2\,kN/m^2$ plus the self-weight of the structure, the load is assumed distributed constantly all along the structure, in this case as for planar RF it is used "Glulam GL24h". The points belonging to the base circle are assumed constrained in the three spatial displacements x, y and z, while the rotations are free. With these data it is analyzed the nexorade taking into account the second order effects, that cannot be neglected due to the high increment of internal actions and displacements (about 29%). The diagram of the internal forces, and the stress state of the elements are reported in the Figure 4.5 and in Figure 4.4, while the maximum values are listed in the Table 4.1.

As a first remark it can be immediately visualized that the in-plane and out-of plane behaviour of the structure is fully coupled, so differently from the planar nexorade in which there weren't axial forces in the frame, here all the elements are in compression. The most interesting part can be seen thanks to the analyzing component "Optimize Cross Section" of *Karamba* that subsequently will be explained in the Section 4.3. In fact using this tool it is possible to visualize where the elements are mostly loaded, i.e. the part in which the element cross-section is bigger, in this particular case but holds for each spatial reciprocal frame, quadrilateral and triangular, the critical

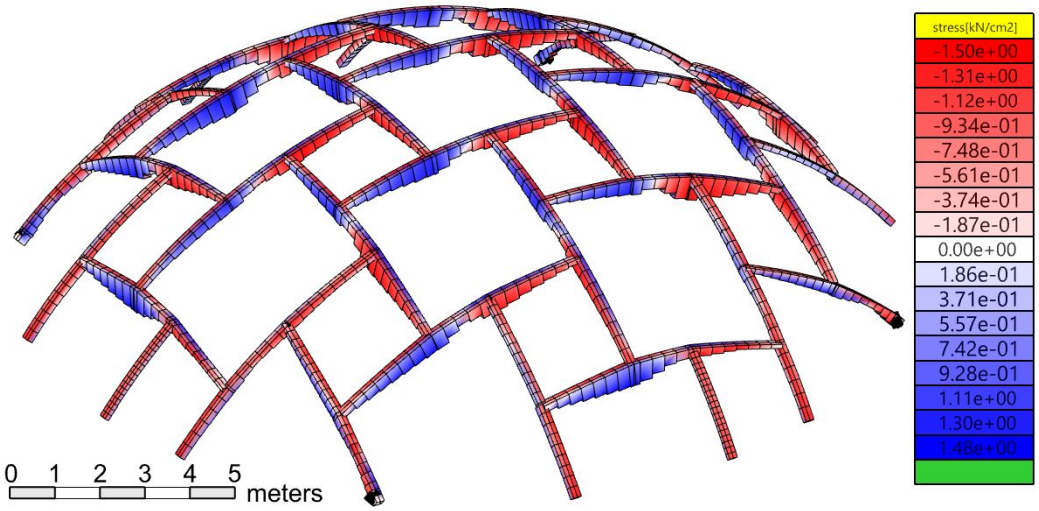

Figure 4.4: Stress state and cross-section visualization

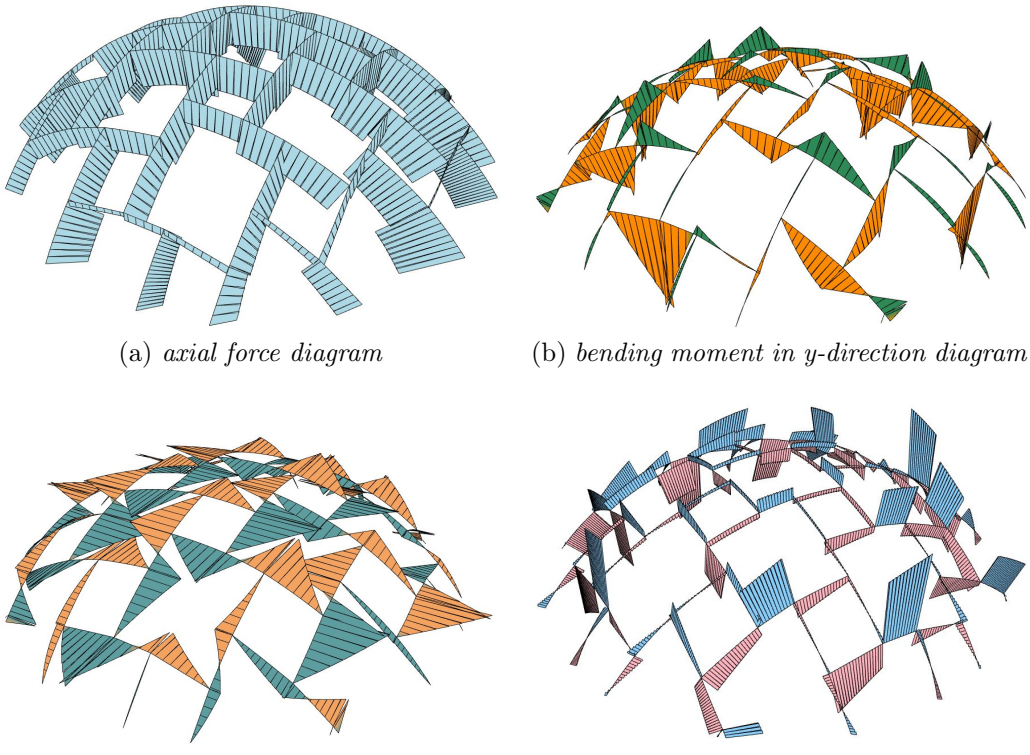

(a) *axial force diagram*

(b) *bending moment in y-direction diagram*

(c) *bending moment in z-direction diagram*

(d) *shear force in z-direction diagram*

Figure 4.5: Internal Forces Diagram

Internal Force	Max	Min
$N_x\,[kN]$	1.99	-105.77
$M_x\,[kNm]$	4.16	-3.66
$M_y\,[kNm]$	43.75	-14.72
$M_z\,[kNm]$	42.83	-42.83
$V_y\,[kN]$	44.63	-65.67
$V_z\,[kN]$	34.77	-34.77

Table 4.1: Maximum and minimum values of internal forces

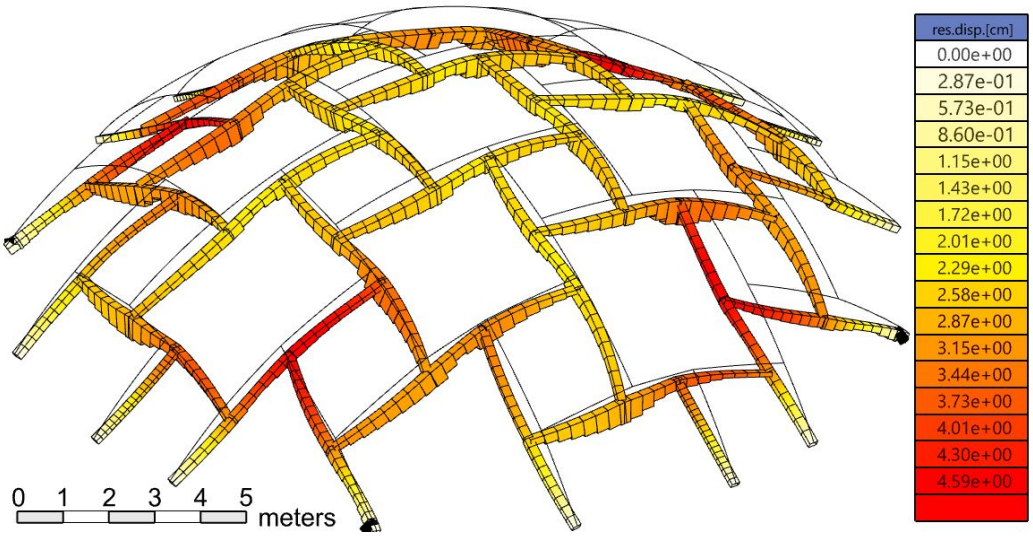

Figure 4.6: Deformed shape

part is the one closer to the connections primarily for two reasons: the axial force (the biggest action) transmitted by the connected element creates a maximum value in the secondary moment M_z, while the shear force coming from always the same element creates a maximum value in the primary bending moment M_y.
For what concern the displacements, in the Figure 4.6 it is reported the deformed shape of the reciprocal frame, the scale of the deformations is higher with respect to the real one in order to highlight the behaviour, with the values reported in the legend is intended the displacement in the space, while the maximum vertical displacement is 3.76cm and the maximum horizontal displacement is 3.51cm. In the Figure 4.6 it can be seen the deflection s-shaped of most of the elements due to the punctual forces transmitted by the connections. In the case in which a glass cover or other fragile type of panels are

choose as a ceiling, the study of the displacement of the frame becomes crucial. In that case the analysis of the deflections must be investigated deeply considering not only the absolute values, but also the relative displacements between the points in which the panels are attached. Although it is not a significant contribution, in that case, the self-weight of the structure doesn't enter in the calculation, because it is an action already present when the ceiling is constructed. A solution to reduce the horizontal displacement of the elements can be the introduction of steel wires between two parallel nexors, such that the two displacements in the opposite directions compensate each other.
The behaviour of triangular macrocell applied to spatial nexorade is quite similar, the biggest differences are in the transmission of axial force in the connection, that due to the inclination between the two elements creates a jump in the axial load diagram of the element, but reduce the horizontal displacement of the element because only a component of the axial force acts in the secondary bending moment M_z.

4.3 Optimization Methods

Differently from what it is done in the Chapter 2 and 3 in which the optimization of the number of cells, so the size of the cells, and the engagement ratio η was performed with a purely practical procedure finding in the global population of the possibilities the less expensive, for the spatial reciprocal frame it has been adopted a model-based optimization tool for *Grasshopper*. This tool called *Opossum* [17] is the first publicly available, model-based optimization tool aimed at architectural design optimization, or more widely aimed to problems that involve time-intensive simulations.
This optimization method was not yet used for nexorades also because looking at the literature the structural optimization was not totally taken into account, the main purpose in the existing literature is the geometrical definition starting from a generic surface. For example the topological optimization done by Godthelp [7] in his thesis is based on the possibility to control manually the eccentricity between elements, similar to the one used by Anastas [1] who impose, using a dynamic interactive physical solver, all the eccentricities equal. While the procedure used by Arup [8] in the design of Rokko Mountain Observatory is the one that closer gets to optimized the total cost, in fact creating the shift base geometry starting from a tridimensional surface the algorithm finds a single combination that would result in the shortest total element length, in other words fixing all the other geometrical parameters the solution obtained results in the flattest shift frame. However Arup didn't do

a sectional modification, imposing a diameter of the elements which remains fixed during the optimization. It can be very interesting also the procedure used by Bavarel[2] in his doctoral thesis where he used a type of black-box optimization population-based that draws its inspiration from natural process and it is called "Genetic Algorithms", however due to the lack of rigor and poor performance the mathematical optimization community regards metaheuristics as "method of last resort"[3]. The procedure used by Bavarel it has been recalled also in the work of Pugnale[15] who has created a simple benchmark in which explains that even if the problem is quite simple the genetic algorithm does not seem to work optimally.
Also the plug-in *Opossum* uses one type of black-box optimization, where with this definition it is intended those optimization problems in which the relationship between variables and performance objective are not explicit by mathematical functions, but by evaluating a parametric model with numerical simulations. In fact *Opossum* is a model-based method, i.e. the algorithm employs surrogate models to guide the search for good solutions, these surrogate models in *Opossum* are "Radial Basis Function" originally proposed by Gutmann(2001)[9] and then developed by Costa & Nannicini(2014)[4] who propose an assessment of model quality using a cross validation scheme, in order to dynamically choose the surrogate model that appears to be the most accurate for the problem. However in order to avoid time consuming processes, also with *Opossum*, it is preferable to use a low number of variables.
In the model used for spherical dome in *Grasshopper*, *Opossum* is used to optimize the size of each macrocell and the engagement ratio η, while for the structural optimization of the cross-section of the reciprocal frame it is used the *Karamba*'s algorithm "Optimize Cross Section". This component takes into account the cross sections load bearing capacity and optionally limits the maximum deflection of the structure. The optimization is done on a finite number of cross-section that is defined by the user, moreover the user passes at the algorithm a first cross-section at which the optimization starts. The procedure followed by *Karamba* is the following:

- Determination of section forces in at least three points along all beams using the initial cross-section
- For each element or given set of elements: selection of the first sufficient entry from cross section
- If no changes were necessary in step two or the maximum number of design iterations is reached, the algorithm stops. Otherwise it returns to step one using the cross sections selected in step two

4.4 Optimized Configuration for 3DRF

Starting from the parameterized geometry constructed above in the Section 4.1 it has been studied the optimized configuration varying η and the size of the macrocell. As for planar nexorades, for optimal configuration is intended the one that minimize the parameter cost that is the only way to weight the reciprocal frame, the connectors and the CLT used as cover.
After a several number of tests and reasoning it has been concluded that the optimal configuration for both quadrilateral and triangular based reciprocal frame is reached for the engagement ratio η equal to 0.5. This result could be expected, because the maximum internal forces are reached due to the transmitted concentrated forces at the connections, but for $\eta = 0.5$ the "secondary" elements intersect the "primary" element in the same position in such a way that the two axial forces are counterbalanced and the secondary moment is generated only by the difference between the two actions (Figure 4.7).

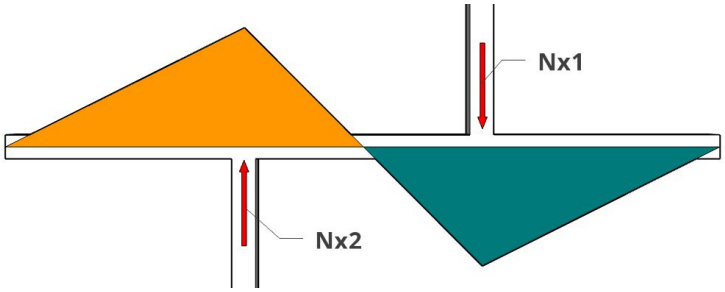

(a) M_x *bending moment for* $\eta \neq 0.5$

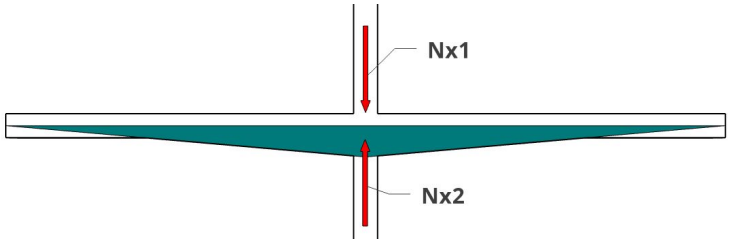

(b) M_x *bending moment for* $\eta = 0.5$

Figure 4.7: M_x bending moment diagrams varying *eta*

So asserted the optimal engagement length they have been developed in details two examples using both the base geometries.

4.4.1 Quadrilateral Based 3D Reciprocal Frame

The optimal configuration in the case of quadrilateral based reciprocal frame is obtained as described in the Section 4.3 with *Opossum* and the "Optimize Cross Section" tool of *Karamba*. As three-dimensional surface it was selected a lowered spherical dome with a radius of 10m and an height of 5m, with an applied live load of 3 kN/m^2. Moreover the tool "Optimize Cross Section" needs a family of cross-section as a input, in this case it was chosen a fixed base of 20cm and a variable height, this solution has been made in order to have a cross-section with a varying height, because it is not feasible to have both width and height varying along the element.
With these data it was performed the numerical optimization considering also the second order effect, the results are reported in the Figure 4.8. From these results it can be seen that the surface interpolating the cost of the structure is negatively sloped towards $\eta = 0.5$ and in the perpendicular direction the surface has a shape of a parabola with a minimum around 2.3m, moreover it is evident that the biggest variation derives from the macrocell size. Anyway the minimum is reached for η equal to 0.5, a macrocell size equal to 2.28m, and with a constant cross-section all over the elements with an height of 10cm. Considering these quantities the cost of the structure is 36421€.

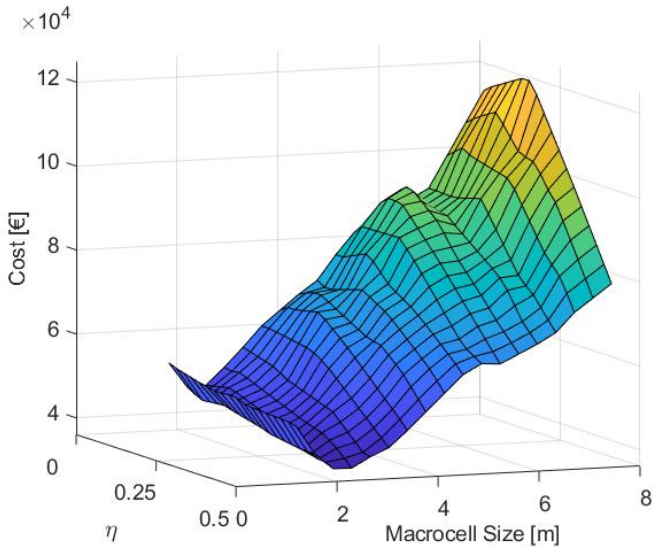

Figure 4.8: Total cost function for quadrilateral based 3DRF

The diagrams of the internal action are reported in the Figure 4.10, while the maximum values are listed in the Table 4.2.

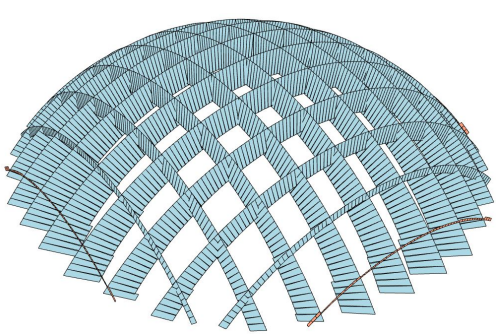

(a) *axial force diagram*

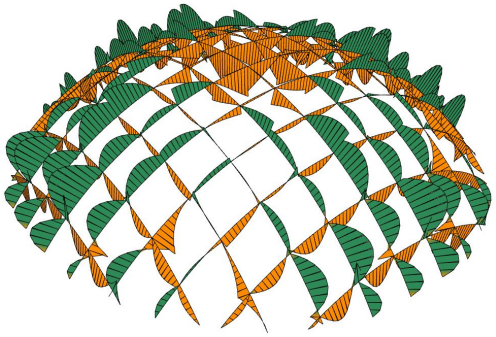

(b) *bending moment in y-direction diagram*

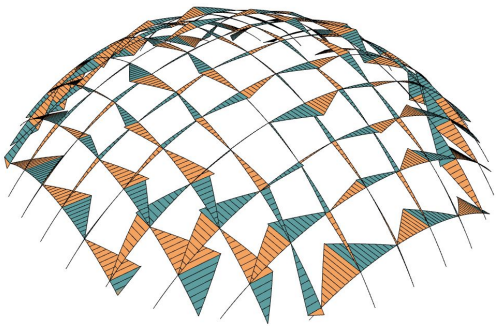

(c) *bending moment in z-direction diagram*

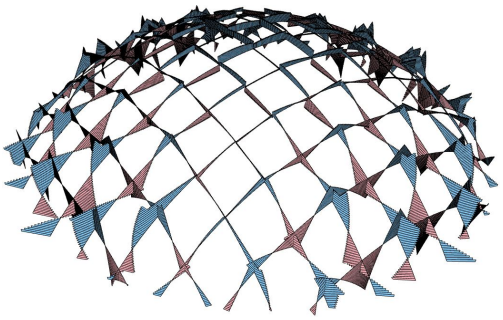

(d) *shear force in z-direction diagram*

Figure 4.10: Internal Forces Diagram

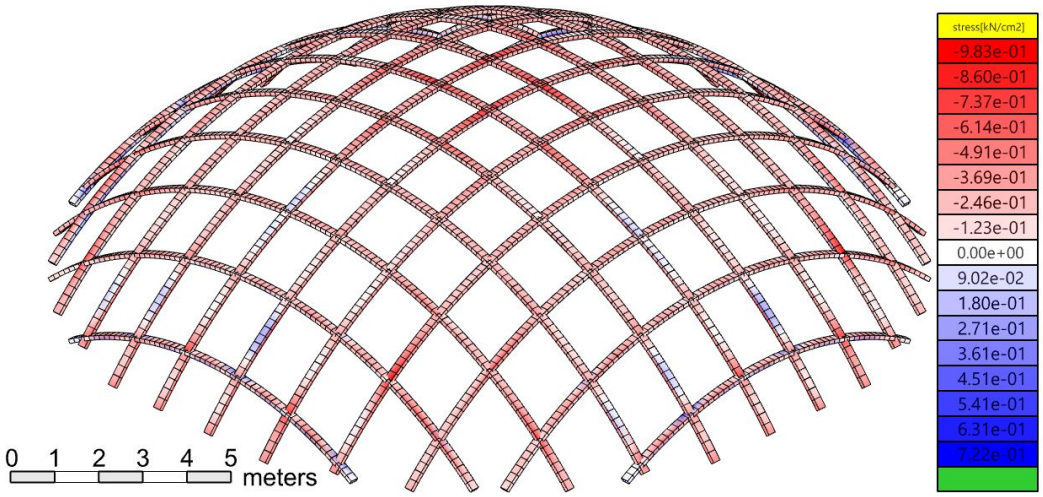

Figure 4.9: Stress state and cross-section visualization

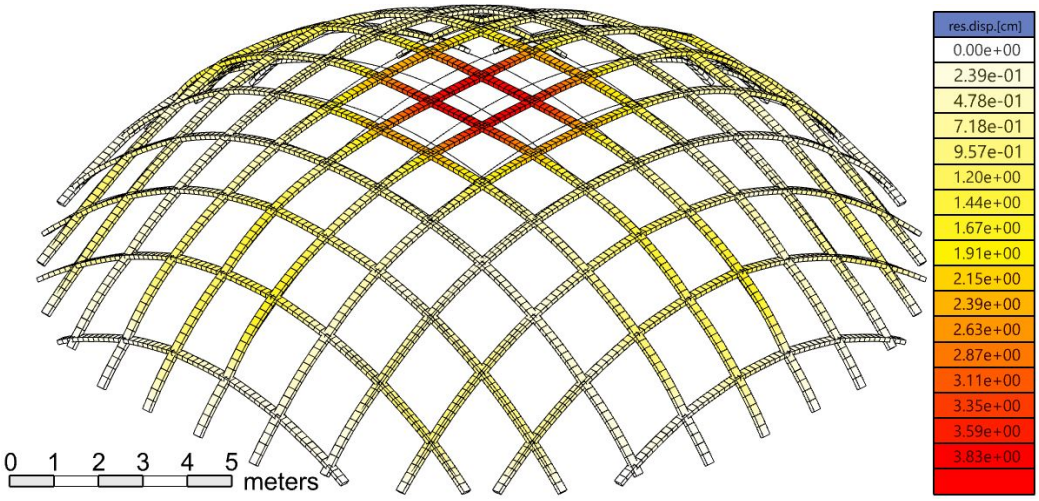

Figure 4.11: Deformed Shape

Internal Force	Max	Min
$N_x\,[kN]$	9.34	-87.80
$M_x\,[kNm]$	0.53	-0.51
$M_y\,[kNm]$	1.87	-1.62
$M_z\,[kNm]$	2.57	-2.53
$V_y\,[kN]$	3.53	-3.28
$V_z\,[kN]$	3.59	-4.76

Table 4.2: Maximum and minimum values of internal forces

Looking at the results coming from *Karamba* it can be derived that in the optimal solution for η equal to 0.5 the preponderant action is the axial one, differently from what it is described for a random eta in the subsection 4.2.1 in which the axial force was still the greatest contribution, but was in the same order of magnitude as the moments and shear forces. It can been also noticed that the last row of elements before the supports are subjected to tension forces, this is due to the axial force in the "vertical" element which tends to open the dome. So at the end the coupled behaviour between flexural and axial is governed by the axial component. Moreover doing a comparison between the results obtained for the planar reciprocal frame and this optimal configuration it can be seen how the bending moments and the shear force are one/two order of magnitude smaller in the case of spatial RF. This observation leads to the conclusion that in this case the cost of the joints is less important in the overall optimization problem.

Focusing instead on the Figure 4.11 it is possible to observe that the deflections are concentrated mainly in the central part of the dome where the elements are more planar and the external load is perpendicular to their. Also the elements at the base, subjected to an high level of axial load and negative bending moment, are experiencing a non-negligible amount of deformation.
As a little remark on the shape of the elements, since all the quantities involved in the design problem are symmetrical, then the final geometry will be symmetrical somehow. In fact the geometry has a central symmetry, this means that not all the elements have different length and shape, but at least an element is repeated equal four time in the overall structure. This should facilitate the production and the construction operations.

4.4.2 Triangular Based 3D Reciprocal Frame

Considering the same quantities used in the previous subsection, it was optimized the usage of triangular based reciprocal frame.
As for the quadrilateral it was performed an optimization with *Opossum* considering also the second order effect. With the values obtained it was constructed the cost surface varying η and the macrocell size. Also for this case in the Figure 4.12 it can be appreciated the slope of the surface in the direction of eta equal to 0.5, and even if it is not accentuated in the plot it exists in the direction of the macrocell size a minimum value around 2.10.

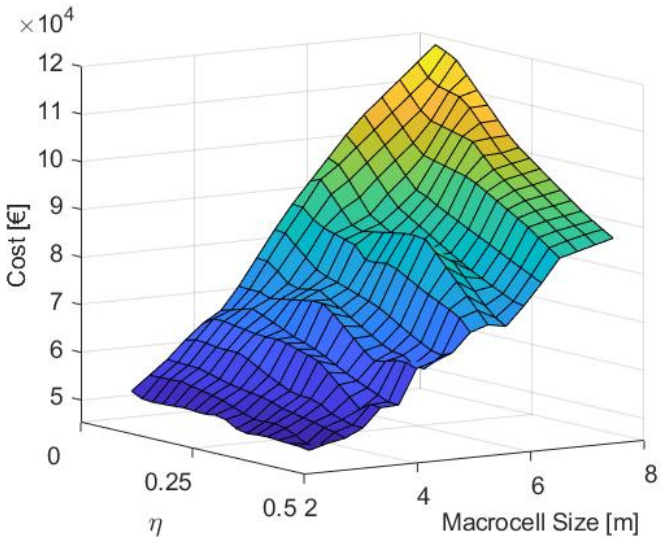

Figure 4.12: Total cost function for triangular based 3DRF

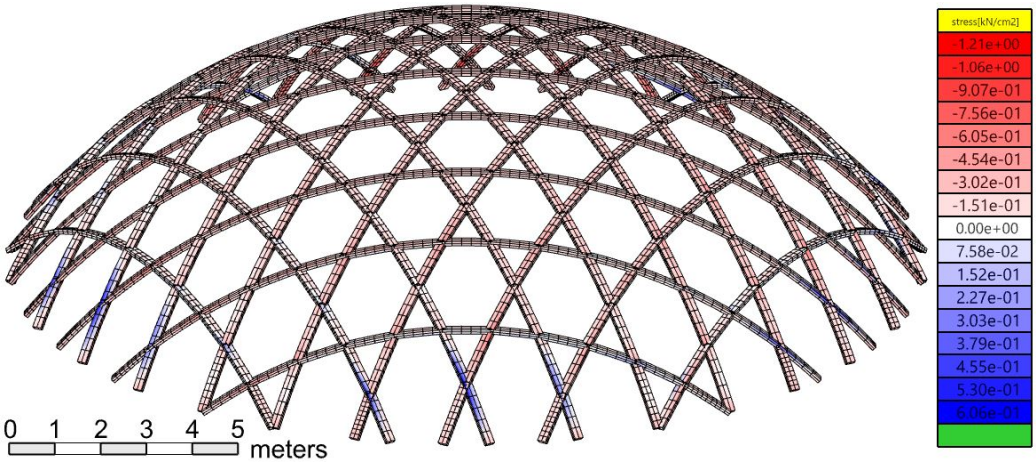

Figure 4.13: Stress state and cross-section visualization

Anyway the global minimum is found for $\eta = 0.5$, macrocell size equal to 2.10 and a constant cross-section for all the elements with an height of 10cm and a base of 20cm. In the optimal case the total cost of the structure is 45228.25€. The remarks that was found for planar nexorades can be repeated also for spatial reciprocal frame, i.e. also for domes the most light configuration and so also the less expensive is the one related to quadrilateral based reciprocal grids, this consideration is probably based on the fact that even if triangles are more rigid to resist at horizontal actions, they have an higher ratio total length on the covered surface.
The relative diagrams of the axial stress state of the sections and the internal forces are respectively reported in the Figure 4.13 and in the Figure 4.14.

Internal Force	Max	Min
$N_x\,[kN]$	1.09	77.90
$M_x\,[kNm]$	0.31	-0.17
$M_y\,[kNm]$	0.87	-1.73
$M_z\,[kNm]$	2.54	-2.54
$V_y\,[kN]$	2.03	-1.70
$V_z\,[kN]$	1.97	-2.55

Table 4.3: Maximum and minimum values of internal forces

As always happens for domes also in this case the preponderant action in coupled behaviour is the axial force that has its maximum in the lowered part of the frame.

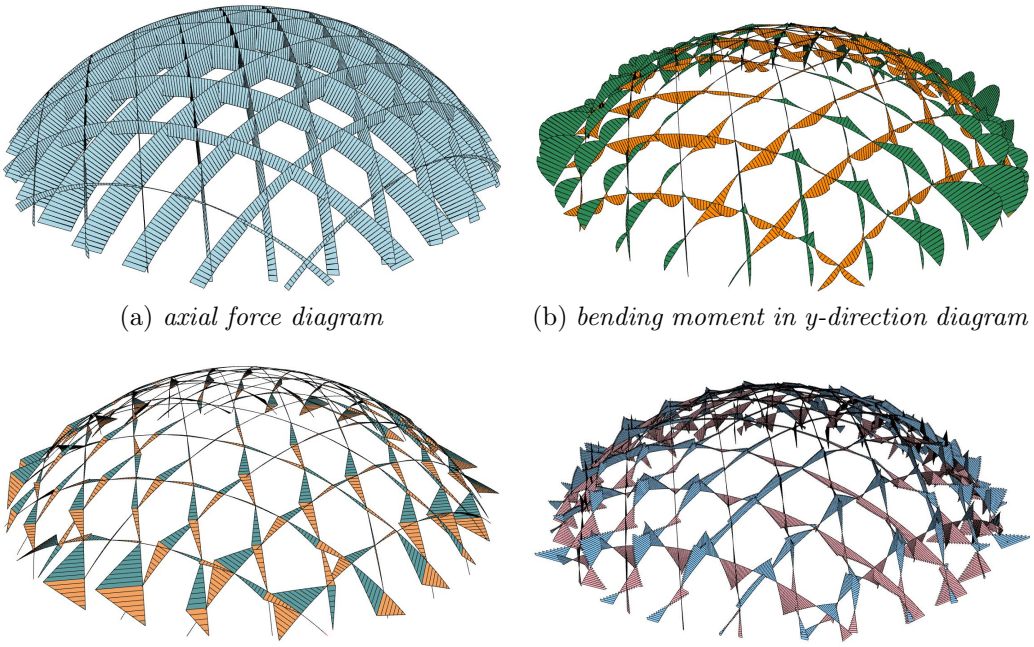

(a) *axial force diagram* (b) *bending moment in y-direction diagram*

(c) *bending moment in z-direction diagram* (d) *shear force in z-direction diagram*

Figure 4.14: Internal Forces Diagram

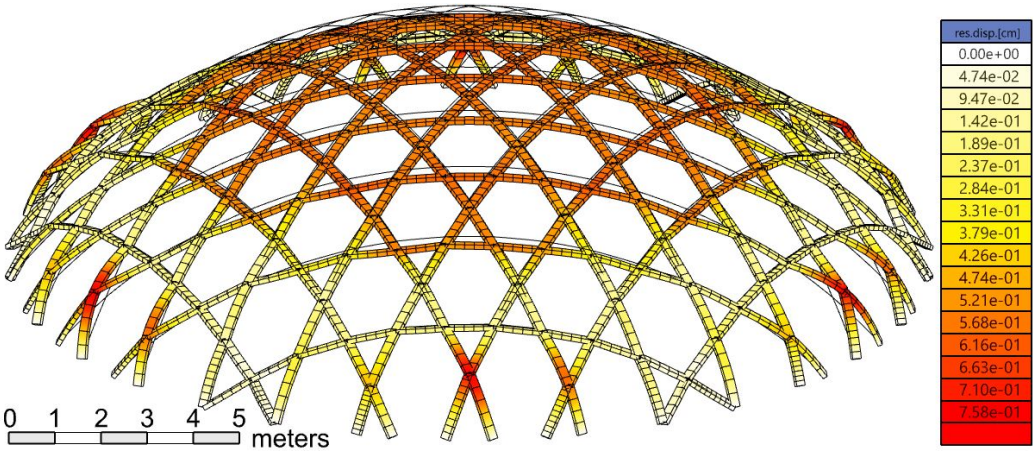

Figure 4.15: Deformed Shape

For what concern the deformed shape plotted in the Figure 4.15 it can been highlighted the lowering of the upper part and the horizontal outward movement due to the push arriving from the axial force. However it has been done a comparison with the quadrilateral based dome, and it has been noticed that the maximum displacements are lower in this case, this thanks to the higher rigidity of the triangular shape in plane.

4.5 Paraboloidal Reciprocal Grids

Even if in this thesis the focus was made in the optimization of the structure giving as data a base surface on which the reciprocal frame was constructed, it is perfectly known from previous literature[16] that considering a uniform distributed vertical load the funicular curve is a parabola. The case of paraboloid surface was therefore studied in order to give another example of an application for reciprocal frames. Keeping the same covered area of the case studied in the Section 4.4 and the same height, it was defined the base parabola.

$$z = -\frac{x^2}{20} + 5 \tag{4.1}$$

Making the revolution around the vertical axis z of this curve it was constructed the paraboloid. Once the surface is defined it can be projected the reciprocal geometry on it. In order to not go too far in the topic of form finding of the surface, the example is focused on the quadrilateral grid, which was the optimal solution until now. Also for this case was made an optimization with *Opossum* varying only the macrocell size, the optimal solution was reached for a macrocll size equal to 2.59m and a constant rectangular cross-section 20x10 cm. The results of this case study are reported in the following figures and table.

Internal Force	Max	Min
$N_x\,[kN]$	-52.05	-76.85
$M_x\,[kNm]$	0.09	-0.09
$M_y\,[kNm]$	0.66	-0.37
$M_z\,[kNm]$	0.50	-0.54
$V_y\,[kN]$	0.25	-0.39
$V_z\,[kN]$	1.76	-1.41

Table 4.4: Maximum and minimum values of internal forces

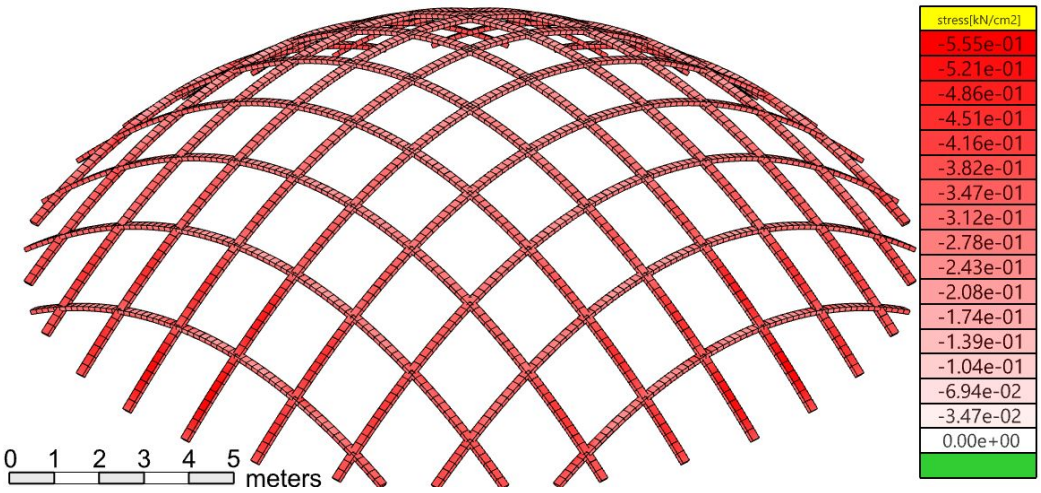

Figure 4.16: Stress state and cross-section visualization for paraboloidal surface

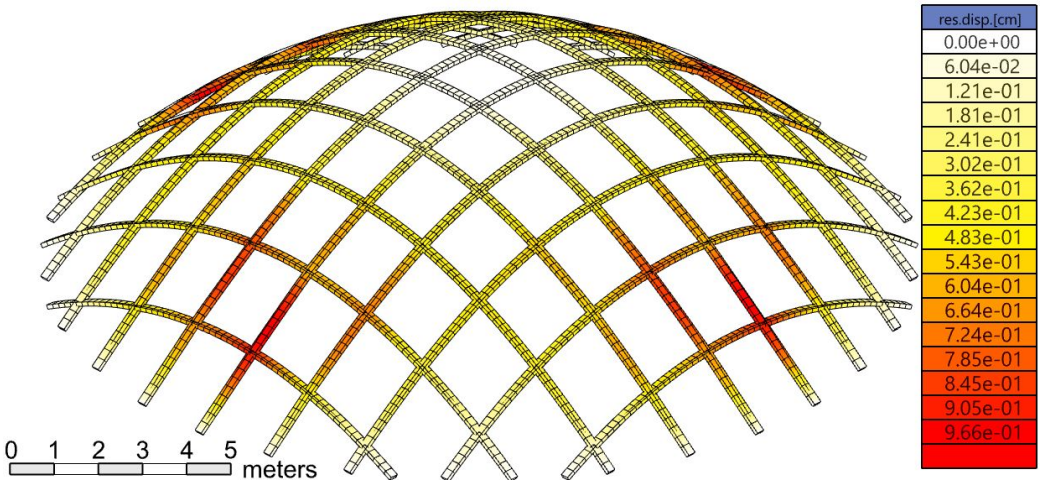

Figure 4.17: Deformed Shape for paraboloidal surface

The most important remark follows what it was said on the funicular curve of the structure, in fact even if funicular behaviour is temporary and an ideal one, because shape and loads inevitably change during the structure life-time, in this specific load case all the points of the cross-sections are only in compression. Moreover, even if they are present, the moments and shear force are very small, almost negligible. This distribution of the stresses helps a lot to reduce the displacements, in fact as it is possible to visualize in the Figure 4.17 the maximum displacements doesn't reach 1cm value. Furthermore, even if it is not accentuated in the deformed shape, differently from the spherical surface, in this case the elements in "vertical" near the supports are subjected to positive bending moment preventing the horizontal outwards displacements.
For what concern the total cost, thanks to the the new shape of the surface the cost is reduced about 5% (total cost 34745€). So at the end considering elements with a minimum base of 20cm used to avoid lateral buckling due to the transmission of axial force, minimum height of 10cm, a circular covered area with a diameter of 20m, an highest point at 5m, and an applied live load of $3kN/m^2$, the optimized solution is reached for quadrilateral based reciprocal frame with an engagement ratio η equal to 0.5 a macrocell size of 2.59m and a paraboloidal surface.

Chapter 5

Conclusions

After a long study on reciprocal frames, which has tried to cover the most notable features of these type of structures, it has been observed that, if the optimal configuration is constrained to comply with the classical shape of the nexorades, a non-optimal solution from structural point of view will be obtained. In fact, except for some special case, the optimal reciprocal configuration degenerates in a regular grid. Considering the reciprocal grid, a comparison can be performed between the already existing techniques, such as the grid composed by primary and secondary beams, and the one in which all the elements are connected by a rigid joint which takes the highest value of loads. In the Figure 5.1 these three configuration are reported.
Assuming that the material used for the three different configuration is more or less the same, the two main cost variables are:

- the cost of the connections
- the cost related to the transportation and installation of the elements

The first variable, the connection's cost, is for sure higher in the third configuration in which the connectors have to sustain the full load, because they are creating a monolithic grid. While the less expensive arrangement is the one with primary and secondary beams, in which the actions transmitted by secondary elements to the primary elements are very small because related to their influence area. Instead for what concern the transportation and installation of the elements, the costs, which are strictly connected to the length of the elements, are exactly the opposite, because in the case with primary beams the maximum length of the elements is equal to the lower span, while for the fixed connections the elements have a length equal to the one of the cell. Moreover if the area to be covered is larger than 13m the transportation of full spanning elements become expensive and expensive, to be then impossible for lengths over 30 meters. So, on the base on these considerations, the

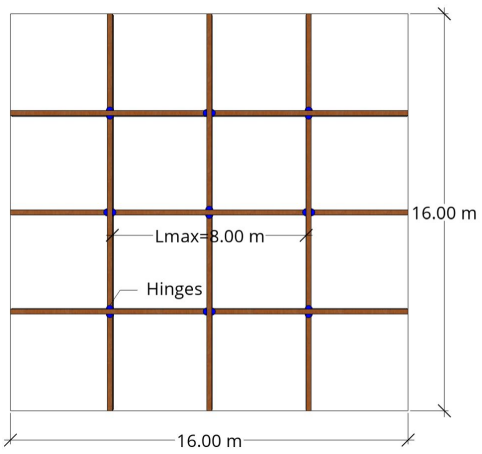

(a) *Reciprocal Grid*

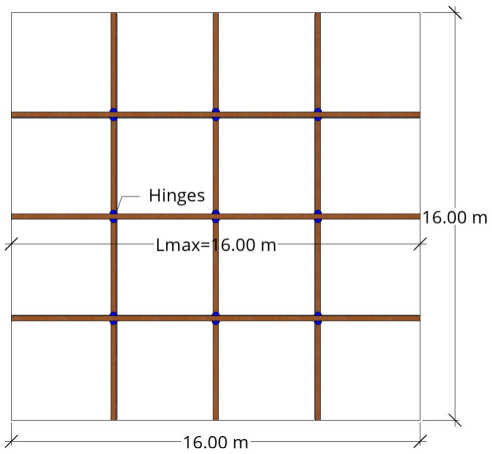

(b) *Primary and secondary beams*

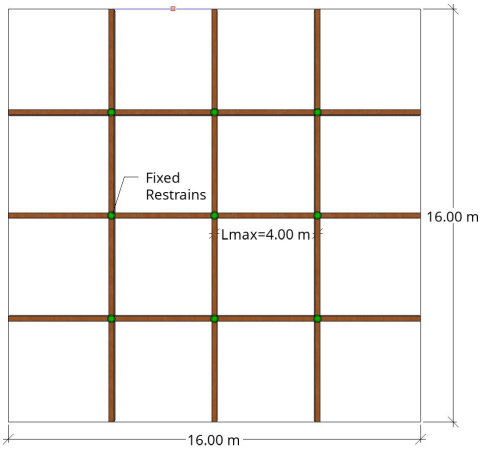

(c) *Fixed connections*

Figure 5.1: Grid Configurations

reciprocal grid always fits in as a solution in the middle, indeed the elements are long twice the cell length and the connections (hinges) transmit a shear force that sometimes become significant. At the end it can be said that the reciprocal frame, with their philosophy of collaboration in order to achieve bigger aims (in the case of structure span lengths), is a valid alternative to the current and largely used systems.
As a conclusion, based on the results highlighted in this thesis, one can infer that: the best way to design a reciprocal frame is to follow the simplicity and the natural energy balance provided by nature's laws. Indeed the structural optimization always reflects these two characteristic in order to achieve the most aesthetic and functional solution.

"La semplicità è la massima raffinatezza"
Leonardo Da Vinci

Appendix A

Stiffness Matrices and Nodal Force Vectors

```
%% Stiffness Matrix of the Macrocell

k1=6/(eta*L)^3+12/(1-eta)^3/L^3;
k2=3/eta/L+4/((1-eta)*L);
k3=3/(eta*L)^2;
k4=3/(eta*L)^3;
k5=-3/(eta*L)^2+6/((1-eta)*L)^2;
k6=12/((1-eta)*L)^3;
k7=6/((1-eta)*L)^2;
k8=4/((1-eta)*L);
k9=2/(1-eta)/L;
K_el=E*I*[ k1,  k3, -k4,  k5,   0,   0, -k4,   0,   0,   0, -k7, -k6,   0,   0,   0,   0;
           k3,  k2,   0,   0,   0,   0,  k5,   0,  k9, -k7,   0,   0,   0,   0,   0,   0;
          -k4,   0,  k1,  k3, -k4,  k5,   0,   0,   0,   0,   0,   0, -k7, -k6,   0,   0;
           k5,   0,  k3,  k2,   0,   0,   0,   0,   0,   0, -k9, -k7,   0,   0,   0,   0;
            0,   0, -k4,   0,  k1,  k3, -k4,  k5,   0,   0,   0,   0,   0,   0,  k7, -k6;
            0,   0,  k5,   0,  k3,  k2,   0,   0,   0,   0,   0,   0, -k9, -k7,   0,   0;
          -k4,  k5,   0,   0, -k4,   0,  k1,  k3,  k7, -k6,   0,   0,   0,   0,   0,   0;
            0,   0,   0,   0,  k5,   0,  k3,  k2,   0,   0,   0,   0,   0,   0,  k9, -k7;
            0,  k9,   0,   0,   0,   0,  k7,   0,  k8, -k7,   0,   0,   0,   0,   0,   0;
            0, -k7,   0,   0,   0,   0, -k6,   0, -k7,  k6,   0,   0,   0,   0,   0,   0;
          -k7,   0,   0, -k9,   0,   0,   0,   0,   0,   0,  k8,  k7,   0,   0,   0,   0;
          -k6,   0,   0, -k7,   0,   0,   0,   0,   0,   0,  k7,  k6,   0,   0,   0,   0;
            0,   0, -k7,   0,   0, -k9,   0,   0,   0,   0,   0,   0,  k8,  k7,   0,   0;
            0,   0, -k6,   0,   0, -k7,   0,   0,   0,   0,   0,   0,  k7,  k6,   0,   0;
            0,   0,   0,   0,  k7,   0,   0,  k9,   0,   0,   0,   0,   0,   0,  k8, -k7;
            0,   0,   0,   0, -k6,   0,   0, -k7,   0,   0,   0,   0,   0,   0, -k7,  k6];
```

```
%% Nodal Force Vector of the Macrocell

P_el=-q*[-L/2*(1+eta); L^2*(eta^2/8-(1-eta)^2/12); -L/2*(1+eta); L^2*(eta^2/8-(1-eta)^2/12);
         -L/2*(1+eta); L^2*(eta^2/8-(1-eta)^2/12); -L/2*(1+eta); L^2*(eta^2/8-(1-eta)^2/12);
          (1-eta)^2*L^2/12;  -L*(1-eta)/2; -(1-eta)^2*L^2/12; -L*(1-eta)/2;
        -(1-eta)^2*L^2/12;  -L*(1-eta)/2;  (1-eta)^2*L^2/12; -L*(1-eta)/2];
```

Figure A.1: Stiffness matrix and nodal force vector of the quadrilateral macrocell

```
%% Stiffness Matrix of the Macrocell

k1=6/(eta*L)^3+12/(1-eta)^3/L^3;
k2=3/eta/L+4/((1-eta)*L);
k3=3/(eta*L)^2;
k4=3/(eta*L)^3;
k5=-3/(eta*L)^2+6/((1-eta)*L)^2;
k6=12/((1-eta)*L)^3;
k7=6/((1-eta)*L)^2;
k8=4/((1-eta)*L);
k9=2/(1-eta)/L;
K_el=E*I*[  k1,  k3, -k4,  k5,   0,   0, -k4,   0,   0,   0, -k7, -k6,   0,   0,   0,   0;
            k3,  k2,   0,   0,   0,   0,  k5,   0,  k9, -k7,   0,   0,   0,   0,   0,   0;
           -k4,   0,  k1,  k3, -k4,  k5,   0,   0,   0,   0,   0,   0, -k7, -k6,   0,   0;
            k5,   0,  k3,  k2,   0,   0,   0,   0,   0,   0, -k9, -k7,   0,   0,   0,   0;
             0,   0, -k4,   0,  k1,  k3, -k4,  k5,   0,   0,   0,   0,   0,   0,  k7, -k6;
             0,   0,  k5,   0,  k3,  k2,   0,   0,   0,   0,   0,   0, -k9, -k7,   0,   0;
           -k4,  k5,   0,   0, -k4,   0,  k1,  k3,  k7, -k6,   0,   0,   0,   0,   0,   0;
             0,   0,   0,   0,  k5,   0,  k3,  k2,   0,   0,   0,   0,   0,   0,  k9, -k7;
             0,  k9,   0,   0,   0,   0,  k7,   0,  k8, -k7,   0,   0,   0,   0,   0,   0;
             0, -k7,   0,   0,   0,   0, -k6,   0, -k7,  k6,   0,   0,   0,   0,   0,   0;
           -k7,   0,   0, -k9,   0,   0,   0,   0,   0,   0,  k8,  k7,   0,   0,   0,   0;
           -k6,   0,   0, -k7,   0,   0,   0,   0,   0,   0,  k7,  k6,   0,   0,   0,   0;
             0,   0, -k7,   0,   0, -k9,   0,   0,   0,   0,   0,   0,  k8,  k7,   0,   0;
             0,   0, -k6,   0,   0, -k7,   0,   0,   0,   0,   0,   0,  k7,  k6,   0,   0;
             0,   0,   0,   0,  k7,   0,   0,  k9,   0,   0,   0,   0,   0,   0,  k8, -k7;
             0,   0,   0,   0, -k6,   0,   0, -k7,   0,   0,   0,   0,   0,   0, -k7,  k6];

%% Nodal Force Vector of the Macrocell

P_el=-q*[-L/2*(1+eta); L^2*(eta^2/8-(1-eta)^2/12); -L/2*(1+eta); L^2*(eta^2/8-(1-eta)^2/12);
         -L/2*(1+eta); L^2*(eta^2/8-(1-eta)^2/12); -L/2*(1+eta); L^2*(eta^2/8-(1-eta)^2/12);
          (1-eta)^2*L^2/12;  -L*(1-eta)/2; -(1-eta)^2*L^2/12; -L*(1-eta)/2;
        -(1-eta)^2*L^2/12;  -L*(1-eta)/2;  (1-eta)^2*L^2/12; -L*(1-eta)/2];
```

Figure A.2: Stiffness matrix and nodal force vector of the triangular macrocell

Appendix B

Tables

B.1 Quadrilateral Reciprocal Frame Solutions

$q = 1[kN/m^2]$					
$L_{tot}\,[m]$	n_{opt}	η_{opt}	$h_{RF}[cm]$	$h_{CLT}[mm]$	$€_{tot}$
8	2	0.425	43.6	60	5962
10	2	0.5	56.6	67	10803
12	3	0.425	58.7	60	17078
14	3	0.5	71.3	62	26005
16	4	0.424	73.4	61	38913
18	4	0.494	86.5	61	55026
20	4	0.5	97.9	67	76278

$q = 2[kN/m^2]$					
$L_{tot}\,[m]$	n_{opt}	η_{opt}	$h_{RF}[cm]$	$h_{CLT}[mm]$	$€_{tot}$
8	2	0.5	54.8	65	7394
10	3	0.437	59.1	60	13581
12	3	0.5	73.5	65	22493
14	3	0.5	86.8	76	35651
16	3	0.5	100.4	87	53433
18	3	0.5	114.0	99	76654
20	4	0.5	118.1	82	106190

$q = 3[kN/m^2]$					
$L_{tot}\,[m]$	n_{opt}	η_{opt}	$h_{RF}[cm]$	$h_{CLT}[mm]$	€$_{tot}$
8	2	0.5	61.7	73	8863
10	3	0.5	68.5	61	16179
12	3	0.5	83.0	73	27528
14	3	0.5	97.8	86	43507
16	3	0.5	112.9	99	65010
18	3	0.5	128.3	112	92976
20	3	0.5	144.1	125	128390

$q = 4[kN/m^2]$					
$L_{tot}\,[m]$	n_{opt}	η_{opt}	$h_{RF}[cm]$	$h_{CLT}[mm]$	€$_{tot}$
8	2	0.5	67.4	80	10137
10	3	0.5	74.9	67	18821
12	3	0.5	90.6	80	31968
14	3	0.5	106.7	94	50420
16	3	0.5	123.0	108	75179
18	3	0.5	139.6	122	107290
20	3	0.5	156.5	136	147860

$q = 5[kN/m^2]$					
$L_{tot}\,[m]$	n_{opt}	η_{opt}	$h_{RF}[cm]$	$h_{CLT}[mm]$	€$_{tot}$
8	2	0.5	72.3	86	11288
10	3	0.5	80.3	72	21242
12	3	0.5	97.1	86	36026
14	3	0.5	114.2	101	56723
16	3	0.5	131.6	116	84437
18	3	0.5	149.2	131	120310
20	3	0.5	167.2	146	165540

B.2 Triangular Reciprocal Frame Solutions

$q = 1[kN/m^2]$					
$L_{tot}\,[m]$	n_{opt}	η_{opt}	$h_{RF}[cm]$	$h_{CLT}[mm]$	$€_{tot}$
8	2	0.5	42.2	65	5951
10	3	0.36	45	60	10551
12	3	0.5	56.7	65	17368
14	4	0.425	58.7	60	26580
16	4	0.418	68.1	70	39173
18	4	0.398	77.6	80	55583
20	4	0.381	87.3	90	76393

$q = 2[kN/m^2]$					
$L_{tot}\,[m]$	n_{opt}	η_{opt}	$h_{RF}[cm]$	$h_{CLT}[mm]$	$€_{tot}$
8	2	0.5	51.6	80	7868
10	3	0.496	56.7	66	14138
12	3	0.459	68.3	83	23783
14	3	0.428	80.1	100	37320
16	4	0.432	82.9	84	55033
18	4	0.414	93.9	97	77603
20	4	0.410	105.5	108	105990

$q = 3[kN/m^2]$					
$L_{tot}\,[m]$	n_{opt}	η_{opt}	$h_{RF}[cm]$	$h_{CLT}[mm]$	$€_{tot}$
8	2	0.5	58.3	90	9407
10	3	0.5	64.1	75	17841
12	3	0.477	77.3	92	29811
14	3	0.451	90.6	111	46494
16	3	0.428	104.1	129	68739
18	3	0.408	117.9	148	97425
20	3	0.395	132.0	167	133470

$q = 4[kN/m^2]$					
$L_{tot}\,[m]$	n_{opt}	η_{opt}	$h_{RF}[cm]$	$h_{CLT}[mm]$	$€_{tot}$
8	2	0.5	63.7	99	10948
10	3	0.5	70.0	82	20826
12	3	0.477	84.3	101	34720
14	3	0.453	98.7	121	53999
16	3	0.432	113.3	141	79603
18	3	0.418	128.4	161	112510
20	3	0.421	144.1	179	153840

$q = 5[kN/m^2]$					
$L_{tot}\,[m]$	n_{opt}	η_{opt}	$h_{RF}[cm]$	$h_{CLT}[mm]$	$€_{tot}$
8	2	0.5	68.2	106	12201
10	2	0.5	86.2	133	23214
12	3	0.479	90.3	108	39255
14	3	0.456	105.7	129	60913
16	3	0.437	121.3	150	89594
18	3	0.440	137.7	170	126450
20	3	0.443	154.5	189	172730

Appendix C

Grasshopper Results for Planar Nexorades

Once I got used to the *Grasshopper* environment we wanted to take a step back and analyze briefly also the planar reciprocal frame with this software.

C.1 Quadrilateral 2DRF

Starting from the example two studied in the subsection 2.3.4, which consider a squared covered area with a span of 16m and an applied live load of $1kN/m^2$, it has been used the "Optimize Cross-Section" tool and as could be expected the elements have a parabola shape, which follows the bending moment diagram, with the biggest rectangle in the correspondence of the connections.

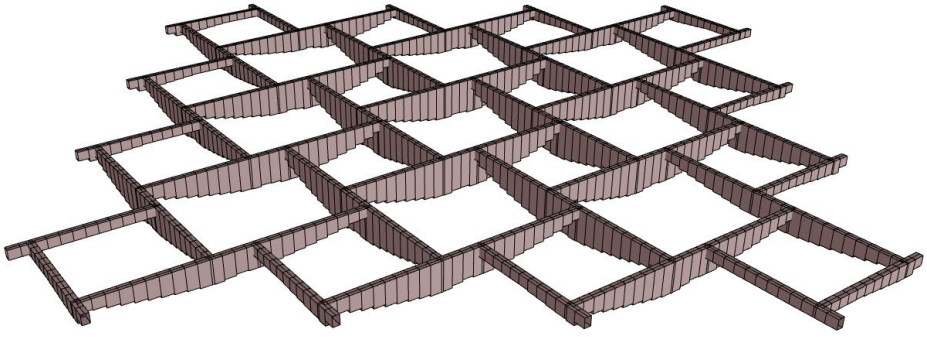

Figure C.1: Cross-section visualization of example 2

Anyway the biggest cross-section has the same parameter of the one founded with *MatLab*, i.e. a base of 15cm and an height of 73cm, but the total cost

is obviously reduced (27673€) thanks to the less amount of timber used and the possibility to correlate at each connection its real shear force.
Moreover it was performed an optimization with *Opossum* and it was found that the best configuration for the software which is probably more accurate with respect to the one obtained with the script. The optimal configuration is different from the one with 4 macrocells for each side found by the script, going back to the Figure 2.11 it can be seen that the minimum is reached by n equal to 4, but it is very close to the one reached by n equal to 3 for $\eta = 0.5$. So probably the material cut from this type of solution by the tool of *Karamba* is more than the one cut from the solution with n equal to 4.

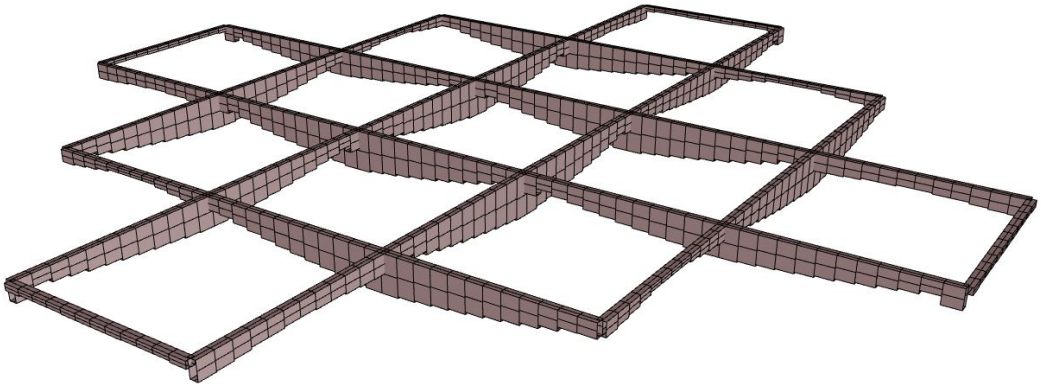

Figure C.2: Cross-section visualization of the optimal planar configiration

The structure reported in the Figure C.2 has a maximum cross-section with a base of 15cm and an height of 87cm, the related total cost amount at 27551€ which is very close to the one obtained with $\eta = 0.424$ and 4 macrocells for each side.

C.2 Triangular 2DRF

Also for the triangular planar reciprocal frame it was repeated an example studied in the subsection 2.3.4, the example 4. Here below for the configuration obtained previously, it is reported in the Figure C.4 the variation of the cross-section along the elements obtained with *Karamba*. With the parametric software it is found a cross-section with a base of 14cm and an height of 67cm very similar to the ones of the script, the total cost it is reduced of 28.7% reaching the value of 27940€.

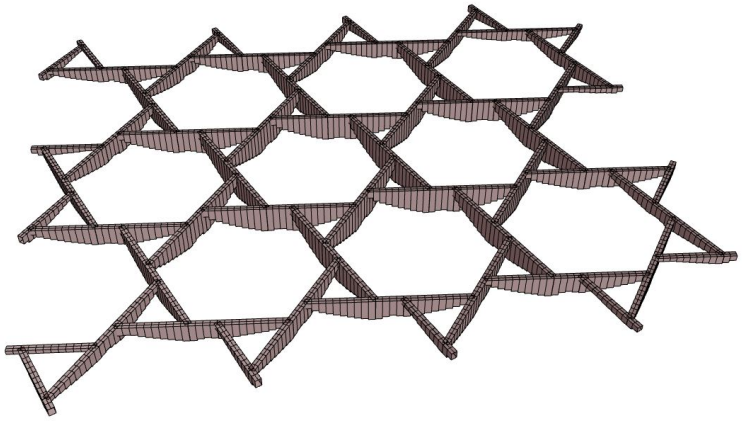

Figure C.3: Cross-section visualization of the example 4

Moreover it was performed the optimization with *Opossum* and it is found a configuration with 4 macrocell along each side as for the example 4, and an engagement ratio equal to 0.5. The biggest cross-section has a base of 14cm and an height of 69cm, and the total cost is equal to 26407€.

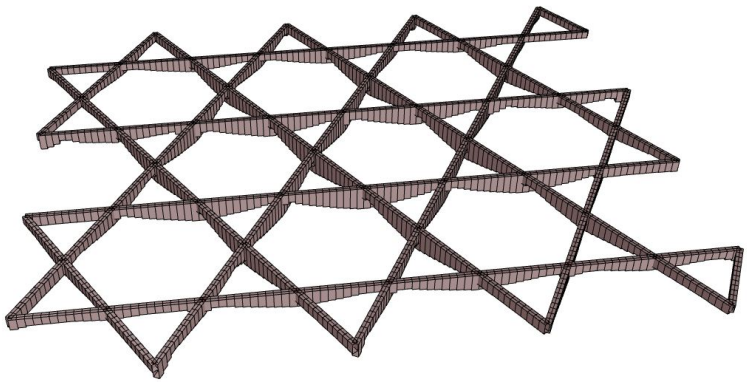

Figure C.4: Cross-section visualization of the optimal planar configuration

Also in this case the two solutions obtained with different method do not match. The missmatch is due to the fact that for eta different from 0.5 there is a length in which the maximum bending moment remains more or less constant, while for the grid solution this length becomes zero and only one section has to sustain the maximum action. So even if the moment related to $\eta = 0.5$ is higher with respect the other solutions, and this fact can be seen in the height of the used section, this effect is more localized and globally the total mass will decrease, while the *Matlab* script consider only the maximum actions whom are higher for the grid arrangement found with the parametric software.

Bibliography

[1] Y. Anastas, L. Rhode-Barbarigos, and S. Adriaenssens. Design-to-construction workflow for cell-based pattern reciprocal free-form structures. *Journal of the International Association for Shell and Spatial Structures*, 57(2):159–176, 2016.

[2] O. Baverel. Nexorades: A family of interwoven space structures. *University of Surrey*, (December):1–323, 2000.

[3] A. R. Conn, K. Scheinberg, and L. N. Vicente. *Introduction to Derivative-Free Optimization*. Society for Industrial and Applied Mathematics, USA, 2009.

[4] A. Costa and G. Nannicini. RBFOpt: an open-source library for black-box optimization with costly function evaluations. *Mathematical Programming Computation*, 10(4):597–629, 2018.

[5] E. Garavaglia, A. Pizzigoni, L. Sgambi, and N. Basso. Collapse behaviour in reciprocal frame structures. *Structural Engineering and Mechanics*, 46(4):533–547, 2013.

[6] S. Gelez, S. Aubry, and B. Vaudeville. Nexorade or reciprocal frame system applied to the design and construction of a 850 m2 archaeological shelter. *International Journal of Space Structures*, 26(4):303–311, 2011.

[7] T. . S. Godthelp. Timber reciprocal frame structures. *Eindhoven University of Technology*, 2019.

[8] K. Goto, R. Kidokoro, and T. Matsuo. Rokko Mountain Observatory. *Arup Journal*, pages 20–26, 2011.

[9] H.-M. Gutmann. A radial basis function method for global optimization. *J Global Optimization*, 2001.

[10] G. T. Houlsby. John Wallis and the Numerical Analysis of Structures. *Nexus Network Journal*, 16(1):207–217, 2014.

[11] R. Mesnil, C. Douthe, O. Baverel, and T. Gobin. Form finding of nexorades using the translations method. *Automation in Construction*, 95(February):142–154, 2018.

[12] O. Popovic Larsen. *Reciprocal Frame Architecture*, volume 369. 2008.

[13] O. Popovic Larsen. Reciprocal Frame (RF) Structures: Real and Exploratory. *Nexus Network Journal*, 16(1):119–134, 2014.

[14] C. Preisinger. PARAMETRIC STRUCTURAL MODELING User Manual for Karamba Version 1.2.2. *Karamba3D*, page 142, 2016.

[15] A. Pugnale. Form-finding of reciprocal structures with gh and galapagos. *https://www.albertopugnale.com/2013/04/05/form-finding-of-reciprocal-structures-with-grasshopper-and-galapagos/*.

[16] L. Todisco and H. Corres Peiretti. IL CONCETTO DI FUNICOLARITA' L'applicazione per il conceptual design di strutture efficienti e versatili. *Structural 201*, (September):1–10, 2016.

[17] T. Wortmann. Opossum : Introducing and Evaluating a Model-based Optimization Tool for Grasshopper. (April), 2017.